

## Supplementary information

Supplementary materials and methods

Supplementary Figures S1 – S11

Supplementary Tables S1 – S5

Supplementary references

## Supplementary materials and methods

### Bacterial and yeast strains

The following bacteria and yeast strains were used: XL2-Blue (*E. coli recA1 endA1 gyrA96 thi-1 hsdR17 supE44 relA1 lac* [F' *proAB lacI<sup>f</sup>ZAM15 Tn10* (Tet<sup>r</sup>) Amy Cam<sup>r</sup>]), BL21-RIL (*E. coli* B F<sup>-</sup> *ompT hsdS*(r<sub>B</sub><sup>-</sup> m<sub>B</sub><sup>-</sup>) *dcm*<sup>+</sup> Tet<sup>r</sup> *gal endA Hte* [*argU ileY leuW* Cam<sup>r</sup>]) and BSY1883 (*S. cerevisiae ade 2-1 his3-11,15 leu2-3,112 trp1Δ ura3-1 can1-100 KanMX6:TetOFF-DIS3, rrp6Δ::URA3*).

### Oligonucleotides, plasmids and cloning

Oligonucleotides and plasmids used are listed in Supplementary Tables S4 and S5, respectively. All restriction enzymes, T4 DNA ligase and CIAP were from Fermentas. All DNA purification kits: DNA Plasmid Mini, DNA Plasmid Midi and Gel-Out were from A&A Biotechnology. PCR reactions were performed with the Phusion DNA polymerase (Finnzymes) or *Pfu* DNA polymerase (Fermentas). Inserts of all the obtained plasmids were sequenced.

The cDNA clones of hDIS3 and hDIS3L were purchased from RZPD (respective imaGenes catalogue numbers: DKFZp667L1817Q and IMAGp998A2015767Q). The hDIS3L cDNA bore one silent mutation, T1221C, which was ignored.

Plasmid pDrK (kindly provided by Dr. Monika Hejnowicz) was generated from pDRIVE (Qiagen). Plasmid pRS72 was created as follows: the TAP-tag coding sequence was PCR-amplified

using the RSZ169 and RZS168 primer pair. The insert was ligated into pDrK digested with *EcoRV*, and subsequently cut out with *XhoI* and *ApaI* and ligated with likewise digested pcDNA5/FRT/TO (Invitrogen). Plasmids pRS201 and pRS255 were generated by annealing oligonucleotide pairs RSZ143-RSZ144 and RSZ132-RSZ133, respectively, and ligating the resulting duplexes with *ApaI*-digested pcDNA5/FRT/TO. Plasmids pHEX1 and pHEX2 were generated by inserting hDIS3 and hDIS3L open-reading frames amplified from RZPD cDNA clones (see above) using primer pairs SLICD3f-SLICD3r and SLICD3lf-SLICD3lr, respectively, into *BamHI* and *XhoI* sites of the pET-28M-6xHis-SUMOTag vector (Lebreton et al, 2008; Malakhov et al, 2004). The sequence and ligation independent cloning (SLIC) technique (Li and Elledge, 2007) was employed. pHEX1 and pHEX2 then served as the PCR templates for all remaining hDIS3 and hDIS3L constructs. Plasmids pHEX3 and pHEX4 were obtained by PCR using primer pairs HD3NFor-HD3NRev and HD3NFor-HD3LNRev with pHEX1 and pHEX2 as templates, followed by ligation of amplification products with T4 DNA ligase in the presence of T4 polynucleotide kinase (NEB) and ATP. Plasmids pHEX5 and pHEX6 were created similarly with the same templates, using HD3CFor-HD3CRev and HD3LCFor-HD3CRev primer pairs, respectively. Plasmids pHEX7 and pHEX13 were generated by site-directed mutagenesis with oligonucleotides D3PINF-D3PINR, using pHEX1 or pHEX3 as templates, respectively. pHEX8 and pHEX14 were obtained by site-directed mutagenesis with oligonucleotides D3RNBF-D3RNBR, employing pHEX1 or pHEX5 as templates. D146N and D487N mutations in hDIS3 were confirmed by PCR with primers SumoF-RTADZ-54, followed by digestion with *MspI* or *Eco32I*, respectively. Plasmids pHEX10 and pHEX15 were created by site-directed mutagenesis with oligonucleotides D3LPINF-D3LPINR, using pHEX2 or pHEX4 as templates, respectively. pHEX11 and pHEX16 were constructed by site-directed mutagenesis with oligonucleotides D3LRNBF-D3LRNBR, employing pHEX2 or pHEX6 as templates. D62N and D486N mutations in hDIS3L were confirmed by PCR with primers SumoF-RTADZ-54, followed by digestion with *MunI* or *AatII*, respectively. Plasmids pHEX9 and pHEX12 were generated by site-directed mutagenesis with primer pairs D3RNBF-D3RNBR and

D3LRNBF-D3LRNBR, using pHEX7 and pHEX10 as templates, respectively. Plasmids pHEX17, pHEX19 and pHEX21 were created in the pRS255, pRS201, and pRS72 vectors, respectively. The coding sequence of hDIS3L was PCR-amplified using the dis3l-tap-fw and dis3l-tap-rv primer pair with pHEX2 as template. The PCR product was gel-purified with the Gel-Out kit and ligated with pDrK digested with *Sna*BI. The ligation reaction mixture was treated with *Sna*BI and transformed into home-made XL2-Blue chemocompetent bacteria (Stratagene). The insert sequence was cut out with *Acc*65I and *Xho*I, gel-purified, and ligated with vectors, which had been similarly digested, dephosphorylated with CIAP and gel-purified. Plasmids pHEX18 and pHEX20 were created like pHEX19 and pHEX21, but the hDIS3 coding sequence was PCR-amplified using the dis3-tap-fw and dis3-tap-rv primer pair with pHEX1 as template. Plasmid pHEX22 was obtained by cloning the hDIS3 open reading frame amplified using the D3COMPL-D3COMPR primer pair and pHEX1 as template into the *Xba*I and *Xho*I sites of the p415 vector. Plasmid pHEX23 was created by cloning the hDIS3L open reading frame amplified with the use of D3LCOMPL-D3LCOMPR primer pair and pHEX2 as template into the *Spe*I and *Xho*I sites of p415. Plasmids pHEX24 and pHEX25 were generated by site-directed mutagenesis of the pHEX25 template, using D3RNBF-D3RNBR and D3PINF-D3PINR oligonucleotide pairs, respectively. Plasmid pHEX26 was constructed by site-directed mutagenesis with oligonucleotides D3RNBF-D3RNBR, employing pHEX25 as a template. Plasmids pHEX27 and pHEX28 were obtained by site-directed mutagenesis with D3RNBF-D3RNBR oligonucleotides, using pHEX18 or pHEX20 as templates, respectively. Plasmid pHEX29 was generated by site-directed mutagenesis with D3PINF-D3PINR oligonucleotide pair with pHEX28 as a template. Plasmid pHEX30 was created by site-directed mutagenesis with D3LRNBF-D3LRNBR oligonucleotides, employing pHEX21 as a template. Plasmid pHEX31 was constructed by site-directed mutagenesis with D3LPINF-D3LPINR oligonucleotide pair with pHEX30 as a template. Plasmids pHEX32 and pHEX33 were constructed by inserting hRRP6 and hRRP41 open-reading frames amplified using primer pairs hRRP6 *Bam*HI FW-hRRP6 FLAG *Not*I RE or hRRP41 *Bam*HI FW-hRRP41 FLAG *Not*I RE with either

pEGFP-N1-PM/SCI-100 plasmid (kind gift from Dr Ger Pruijn) or oligo-dT-primed cDNA from HEK293T cells as templates, respectively, into *Bam*HI and *Not*I sites of pcDNA5/FRT/TO vector (Invitrogen). Plasmid pHEX34 was generated by mutagenesis using hD3Fup-hD3Fdown primer pair and pHEX22 as a template. Plasmid pHEX35 was obtained by cloning the hDIS3L open reading frame amplified using the D3LCOMPL-hD3LFrev primer pair and pHEX23 as template into the *Spe*I and *Xho*I sites of the p415 vector.

### **Cell culture and transfection**

HeLa or HEK293 Flp-In T-REx (Invitrogen) cells were cultured as monolayers in Dulbecco's modified Eagle's medium (D-MEM, Gibco) supplemented with 10% foetal bovine serum (FBS; Gibco) and antibiotics (Penicillin-Streptomycin; Sigma-Aldrich) at 37°C in a 5% CO<sub>2</sub> humidified atmosphere. The stable HEK293 Flp-In T-REx cell lines obtained in this study using the Flp-In system (Invitrogen) were grown in DMEM supplemented with Tet-free FBS (Autogen Bioclear or Invitrogen) and hygromycin B (100 µg/ml) and blasticidin (10-15 µg/ml; both from Invitrogen). Transfections were done with either Lipofectamine2000 (Invitrogen) or polyethyleneimine (PEI; Euromedex) according to the manufacturers' guidelines.

The stable inducible cell lines overexpressing different versions of hDIS3 and hDIS3L as well as hRRP6 and hRRP41 were generated with the use of the Flp-In™ T-REx™ system (Invitrogen) according to the protocol of the manufacturer.

### **RNAi and cell viability assays**

siRNA-mediated knockdown was done essentially as described in (Preker et al, 2008). Briefly, 6x10<sup>5</sup> HeLa cells were seeded in 100 mm plates. 24 h later they were transfected with 20 nM siRNA using 10 µl SilentFect (BioRad) After 60 h, the cells were re-transfected using 10 µl of Lipofectamine2000 (Invitrogen). 48 h later, cells were harvested. siRNA targets are listed in Supplementary Table S4.

Cell viability was determined by running two depletion experiments in parallel and counting cells twice, using a “Countess® Automated Cell Counter” (Invitrogen), 2 or 4 days, respectively, after the second transfection.

### **Reverse transcription, quantitative PCR and Northern blotting**

1 µg of DNaseI-treated RNA extracted from HeLa cells was reverse transcribed by using 20 pmol of an anchored dT primer (Supplementary Table S4) and Superscript II reverse transcriptase (Invitrogen) according to the manufacturer’s instructions in a final volume of 20 µl. 1/40 of a cDNA reaction was mixed with Platinum SYBR Green (Invitrogen) and 2x2.5 pmol of oligonucleotides (Supplementary Table S4) in a final volume of 20 µl and used for real-time PCR analysis on a Mx3005P machine (Stratagene) using an annealing temperature of 59°C. Negative controls lacking Superscript II reverse transcriptase showed a negligible background. All data were normalized to GAPDH mRNA.

Northern blotting was done by customary methods. 10 µg of total HeLa RNA were separated on a 7% denaturing polyacrylamide gel followed by electroblotting onto a Hybond N+ membrane (GE Healthcare). Alternatively, 10 µg of total yeast RNA were separated on a 1% denaturing agarose gel containing 0.925% formaldehyde and immobilized on the same type of membrane by overnight capillary transfer in 20xSSC (3 M NaCl, 0,3 M sodium citrate) The blots were handled according to standard procedures and probed either at 42°C with oligonucleotide probes directed against human 5.8S rRNA or yeast SRP RNA (scR1) (Supplementary Table S4) or at 65°C with probes against hDIS3 or hDIS3L, generated by digestion of .pHEX18 or pHEX19 plasmid construct with *Acc65I/EcoRI* or *Acc65I/HindIII* restriction enzymes, respectively.

### **Heterologous expression and purification of proteins**

Full-length wild-type yeast Dis3p was purified as described in (Lebreton et al, 2008). For purification of full-length and truncated hDIS3 and hDIS3L versions, *E. coli* BL21-CodonPlus-RIL strain (Stratagene) was transformed with appropriate plasmids (pHEX1-pHEX16). Transformants were

grown at 37 °C in 1 l of LB medium supplemented with kanamycin (30 µg/ml) and chloramphenicol (34 µg/ml), following inoculation from a pre-culture at  $OD_{600} \approx 0.1$ . When  $OD_{600}$  reached 0.45–0.5, the cultures were cooled to 16 °C for 30 min and protein expression was induced by the addition of isopropyl  $\beta$ -D-thiogalactopyranoside (Sigma-Aldrich) to a final concentration of 1 mM. Cultures were then incubated overnight at 16 °C. After centrifugation, pellets were resuspended in buffer 1 (20 mM Tris-HCl, pH 8.0; 200 mM NaCl; 10 mM imidazole; 10 mM 2-mercaptoethanol) and lysed by sonication in a Bioruptor device (Diagenode), followed by ultracentrifugation at 32000 rpm for 45 min in a Beckman 35 Ti rotor. Native protein extracts were loaded on an Ni-NTA Superflow Cartridge 1 ml column (QIAGEN) compatible with the Äkta FPLC purification system (GE Healthcare). The column was washed with buffer 1 and then with buffer 2 (20 mM Tris-HCl, pH 8.0; 1 M NaCl; 10 mM imidazole; 10 mM 2-mercaptoethanol). After re-equilibration with buffer 1, proteins bound to the resin were eluted using buffer 3 (20 mM Tris-HCl, pH 8.0; 200 mM NaCl; 600 mM imidazole; 10 mM 2-mercaptoethanol). Fractions of the eluate were combined and dialysed overnight at 4 °C against 2 l of buffer 1 in the presence of 6×His-tagged SUMO protease (10 µg/ml). After dialysis, the protein mixture was subjected to a second round of purification on an Ni-NTA Superflow Cartridge 1 ml column, including the collection of purified protein (devoid of 6×His-SUMOTag) in the flowthrough fraction (in buffer 1) and elution of 6×His-SUMOTag along with 6×His-SUMO protease in buffer 4 (20 mM Tris-HCl, pH 8.0; 1 M NaCl; 600 mM imidazole; 10 mM 2-mercaptoethanol). Proteins were further purified by size-exclusion chromatography on either Superdex 200 10/300 GL (for FL and Cterm protein versions) or Superdex 75 10/300 GL (for Nterm protein versions) column (GE Healthcare). The final elution was always performed using 10 mM Tris-HCl, pH 8.0 with 150 mM NaCl. Finally, glycerol was added to the protein preparations (30% final concentration), which were stored at –80 °C. The purity of the proteins was assessed by electrophoresis in NuPAGE gels (Invitrogen).

### **Purification of FLAG-tagged proteins from yeast following complementation assays**

Pelleted yeast cells obtained from 4 liters of culture at logarithmic phase (-LEU medium) were resuspended in 5 ml of lysis buffer (40 mM Hepes-KOH, pH 8.0; 75 mM NaCl for hDIS3 or 150 mM NaCl for hDIS3L; 1 mM DTT) and frozen in liquid nitrogen. Frozen pellets were broken in laboratory blender with dry ice for 8 minutes, and subsequently 5 ml of lysis buffer with 2 x protease inhibitors cocktail. Following ultracentrifugation at 32000 rpm for 90 min in a Beckman 35 Ti rotor lysates were dialysed against 2 liters of dialysis buffer (40 mM Hepes-KOH, pH 8.0; 75 mM NaCl for hDIS3 or 150 mM NaCl for hDIS3L; 1 mM DTT; 1 mM PMSF; 20  $\mu$ M benzamidine hydrochloride; 25% glycerol (w/v)) for 3 hours in 4°C. 14 ml of dialysed protein extract from each strain was obtained. Half of each extract (7 ml) was incubated overnight in 4°C with 150  $\mu$ l of Agarose anti-FLAG (M2) beads (Sigma) with rotation. After binding beads were collected and washed twice with 10 ml of LS buffer (10 mM Tris-HCl, pH 7.4; 150 mM NaCl; 1 mM DTT; 1 mM PMSF; 1 x protease inhibitors cocktail), then with 10 ml of HS buffer (as LS, but with 1 M NaCl) and again twice with 10 ml of LS buffer. Finally, beads with bound proteins were suspended in 50  $\mu$ l of LS buffer, mixed with an equal volume of 2x Laemli buffer (0.125 M Tris-HCl, pH 6.8; 4% SDS; 20% glycerol; 10% 2-mercaptoethanol, 0.004% bromphenol blue) and analyzed in SDS-PAGE.

### **Purification of TAP-tagged proteins from HEK293 Flp-In T-REx cells for proteomic analyses**

Induced HEK293 Flp-In T-Rex cells were collected by pipetting and washed with PBS. Cell pellets were weighed and, assuming a density of 1.25 g/ml, suspended in one pellet volume of buffer 2xA. Then two pellet volumes of buffer A were added and the cells were disrupted by sonication with a Bioruptor device. Disrupted cells were centrifuged at 1600xg for 10 min to discard the cell debris and undrupted cells. The supernatant was collected and ultracentrifuged at 32000 rpm for 40 min in a Beckman 35 Ti rotor. The pellet containing the insoluble protein fraction was discarded and the supernatant containing soluble fraction was collected. 1/100 volume of 10% Triton X-100 was added and the solution was purified on IgG-Sepharose (Amersham Pharmacia). The resin (50  $\mu$ l/g pellet) was

placed in a PolyPrep column (Biorad) and equilibrated with buffer A. The protein solution was loaded on the column and incubated for 2 h at 4°C with rotation. After binding, the column was drained, washed twice with buffer A and twice with buffer B. After draining of the last wash, the resin was resuspended in buffer B (200 µl/g pellet) and TEV protease was added, followed by incubation at room temperature for 2 h. The column was then drained and washed twice with the same volume (*i.e.* 220 µl per gram of initial cell pellet) and the eluate was stored. Subsequently, proteins in the eluate were precipitated using the PRM reagent (Marshall et al, 1995) and the pellet was subjected to MS analysis to identify purified proteins.

The entire procedure was performed with different NaCl concentrations for the two human DIS3 paralogs knowing that binding of hDIS3 to the core is dependent on ionic strength. Thus two types of buffer A were used, both containing 10 mM Tris-HCl, pH 8.0; 1 mM DTT; 1 mM PMSF and 1x protein inhibitor cocktail, with A1 also containing 50 mM NaCl for hDIS3-TAP and A2 – 125 mM NaCl for hDIS3L-TAP. Respective buffers B1 and B2 were similar, but with the addition of 0.5 mM EDTA.

#### **Substrate and molecular weight marker preparation for *in vitro* biochemical assays**

ss17-A<sub>14</sub>, ss17-A<sub>30</sub> and ss44 oligoribonucleotides (Invitrogen) were purified by electrophoresis in a 10% polyacrylamide gel containing 8 M urea. Oligoribonucleotides were detected by ultraviolet shadowing, excised and the RNAs were eluted overnight at 25°C in a buffer containing 100 mM Tris-HCl, pH 8.0; 12.5 mM EDTA; 150 mM NaCl; 1% SDS and an equal volume of phenol:chloroform (1:1; v:v).

5'-end labelling of substrates was performed with T4 polynucleotide kinase (NEB) and [ $\gamma$ -<sup>32</sup>P]ATP (GE Healthcare) according to the manufacturer's instructions.



3'-end labelling was performed with [<sup>32</sup>P]pCp, either home-made (prepared by incubating cytidine 3'-monophosphate with [ $\gamma$ -<sup>32</sup>P]ATP in the presence of T4 polynucleotide kinase) or purchased from Perkin-Elmer, and T4 RNA ligase (NEB), according to the manufacturer's instructions.

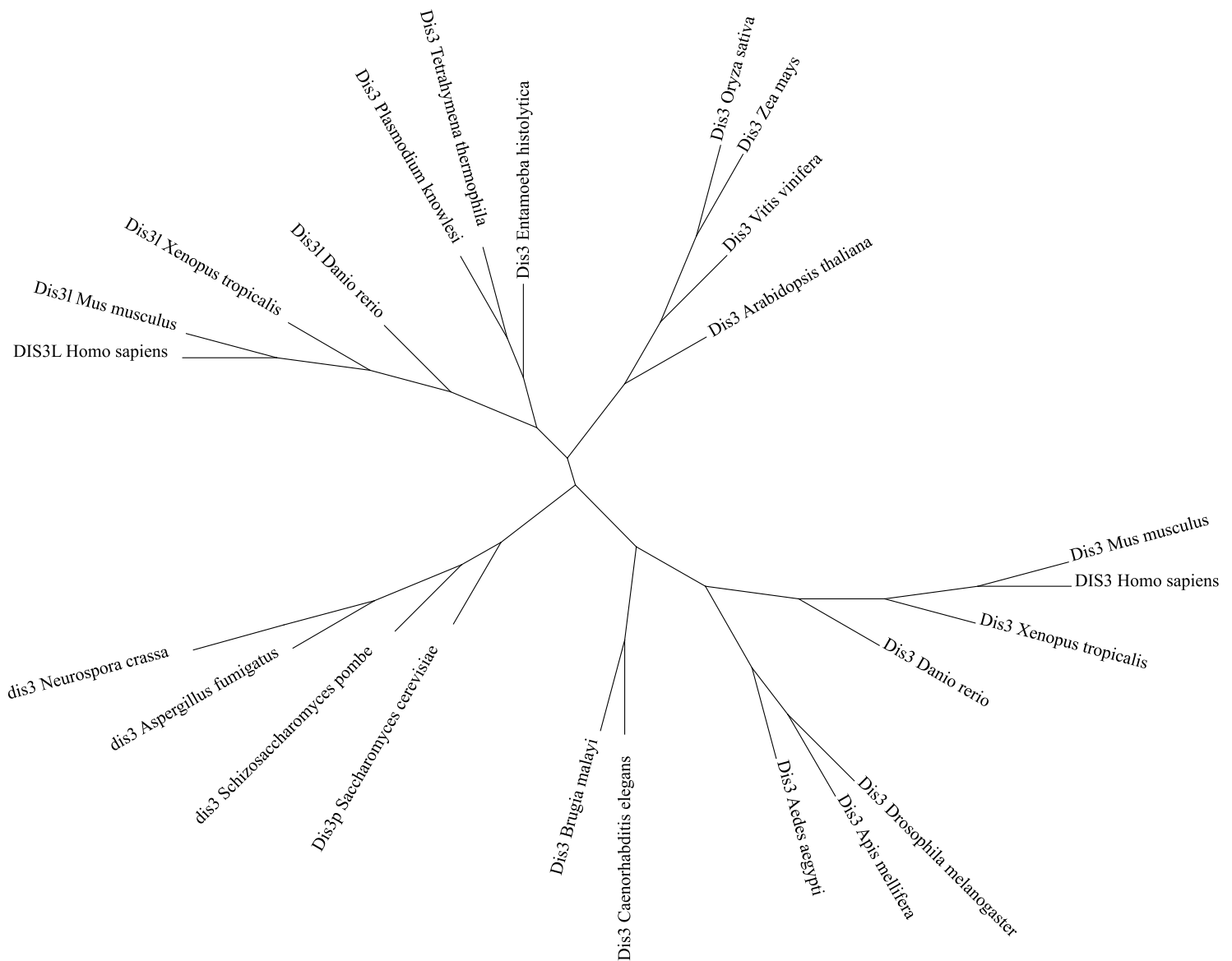
Circularized ss17-A<sub>14</sub> substrate was prepared by incubating 150 pmol of the oligoribonucleotide with 250 pmol of unlabelled ATP and 4 pmol of [ $\gamma$ -<sup>32</sup>P]ATP in a buffer containing 50 mM Tris-HCl, pH 8.0; 10 mM MgCl<sub>2</sub>; 10 mM DTT, in the presence of both T4 polynucleotide kinase and T4 RNA ligase.

All labelled RNA substrates were purified following electrophoresis in 10-20% denaturing polyacrylamide gels with 8 M urea as described above.

3 nt-long molecular weight marker was generated by digestion of 5'-labelled complementary oligoribonucleotide (see Supplementary Table S4) with RNase T1 (Roche).



B

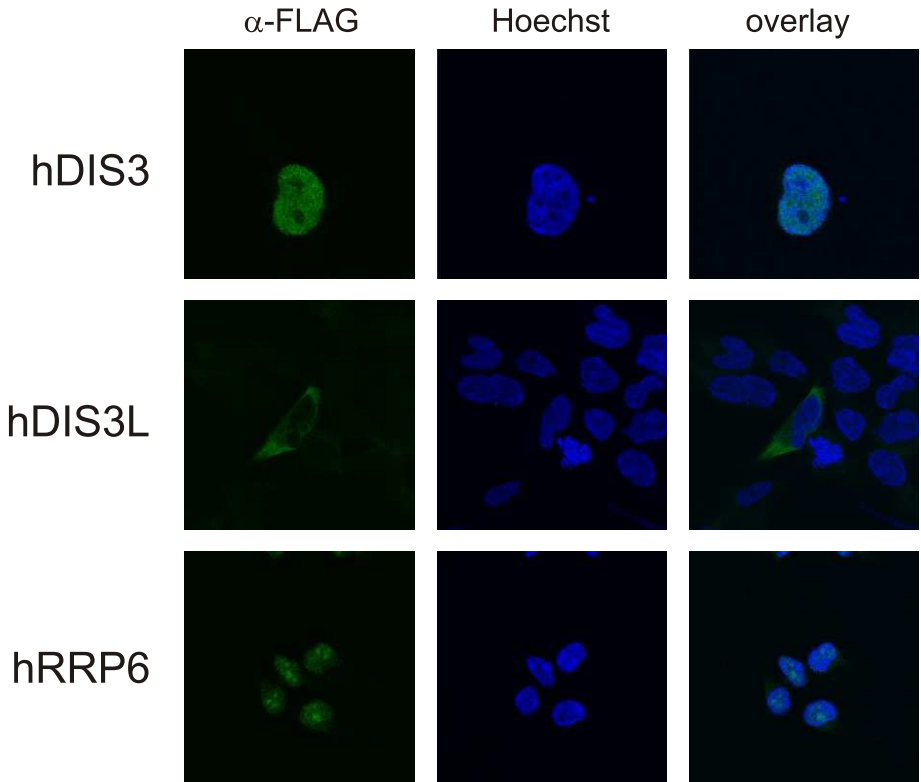


**Supplementary Figure S1. *In silico* analysis of hDIS3 and hDIS3L amino acid sequence and evolutionary history.**

(A) Full sequence alignment of yeast Dis3p (Dis3p\_Sc) and its human (DIS3\_Hs, DIS3L\_Hs) and mouse (Dis3\_Mm, Dis31\_Mm) counterparts. Conserved amino acid residues are marked in grey. Positions of functional domains are indicated above the alignment. Residues involved in the coordination of divalent cations in the catalytic centers of PIN and RNB domains are marked in red and residues potentially participating in substrate binding are marked in blue.

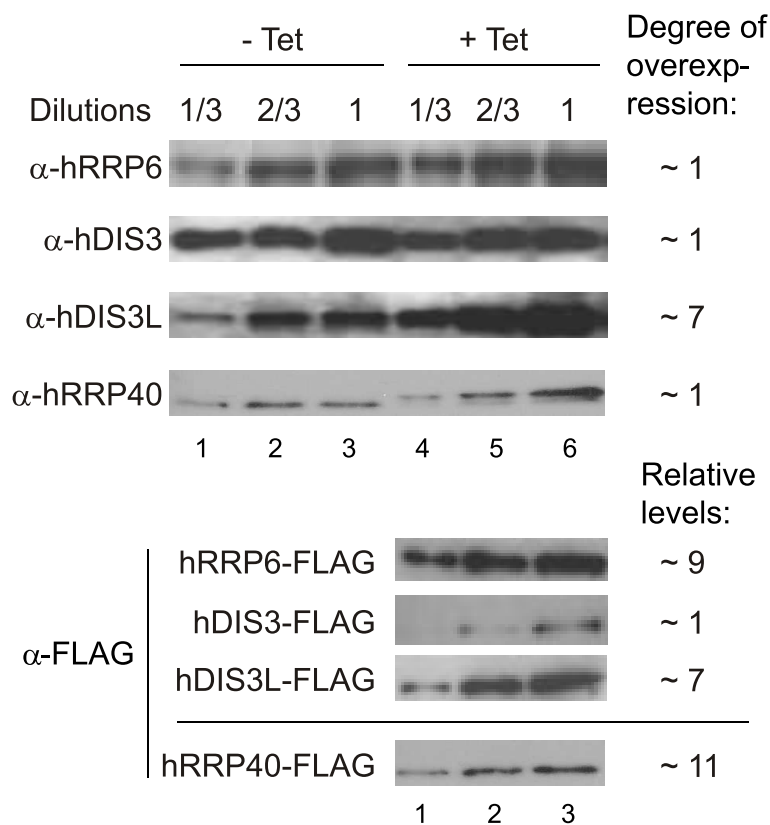
(B) Paralogy of the Dis3 gene in vertebrates. Maximum likelihood phylogenetic tree of the Dis3 protein family.





**Supplementary Figure S3. Intracellular localization of FLAG-tagged hDIS3, hDIS3L and hRRP6 in HEK293 Flp-In T-REx cells.** Stable lines were treated with tetracycline and subjected to  $\alpha$ -FLAG antibody staining and confocal microscopy. Hoechst stained nuclei were overlaid as indicated.

A



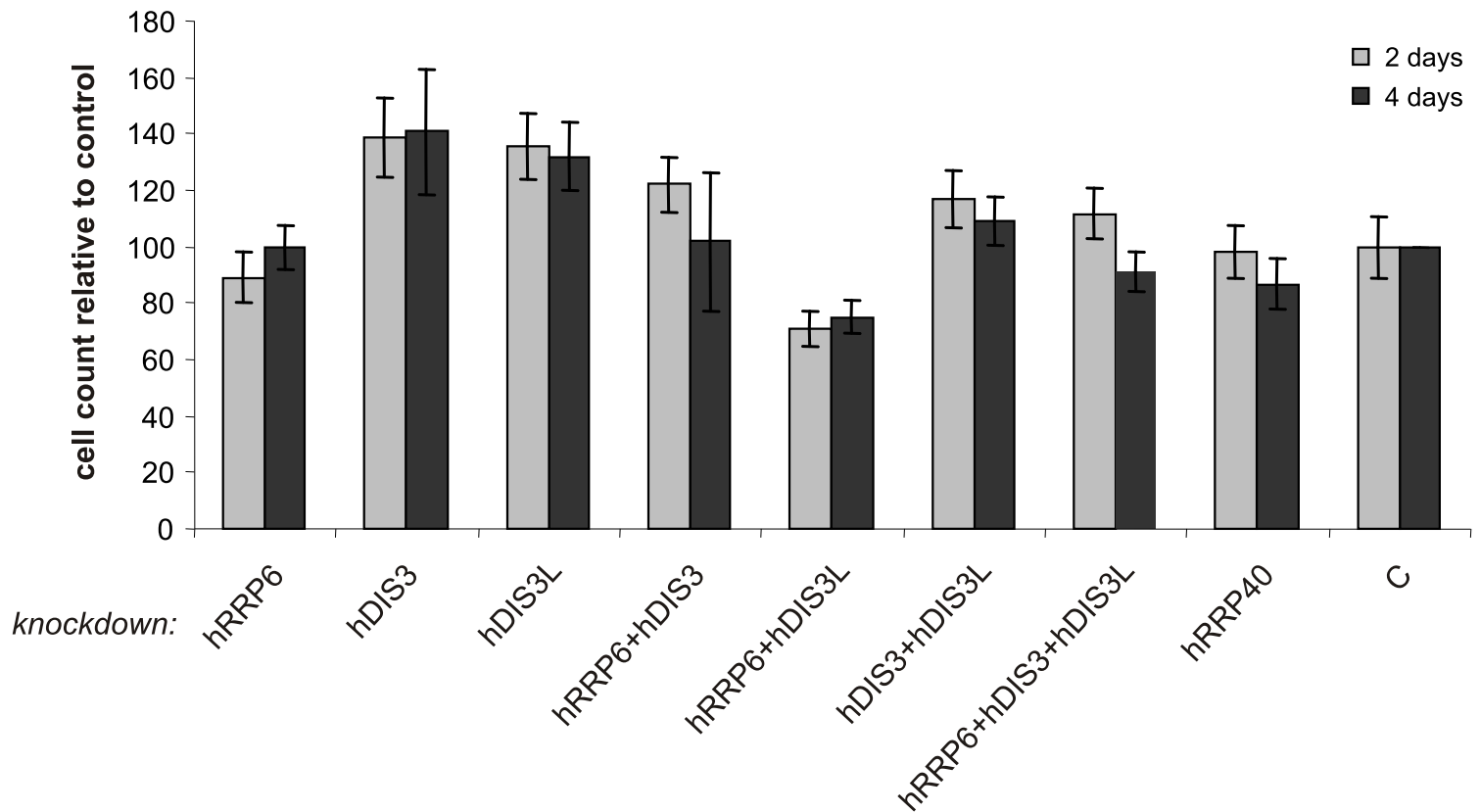
B

Relative cellular levels:	
hRRP6	~ 9
hDIS3	~ 1
hDIS3L	~ 1
hRRP40	~ 11

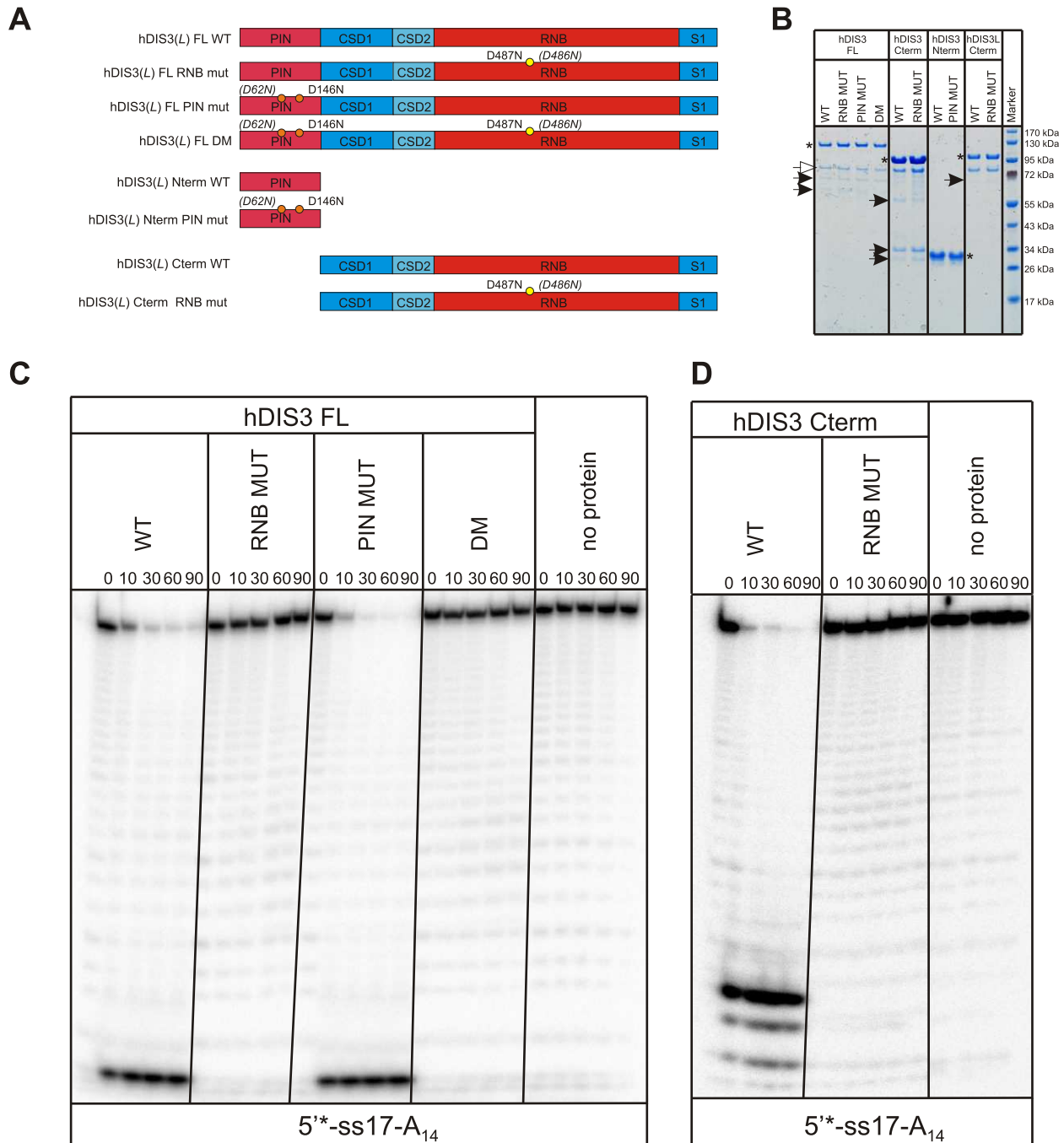
**Supplementary Figure S4. Western blotting analysis of cell extracts from uninduced and Tet-induced hRRP6-FLAG, hDIS3-FLAG, hDIS3L-FLAG and hRRP40-FLAG HEK293 Flp-In T-REx cell lines.**

(A) upper panel: the indicated dilutions of extracts were probed with antibodies recognizing endogenous versions of hRRP6, hDIS3, hDIS3L and hRRP40. The degree of factor overexpression (indicated on the right) was calculated by quantifying (using Quantity One; BioRad) the average ratio of the three signals in the Tet-induced extracts (containing both endogenous and FLAG-tagged proteins) and the three signals in the uninduced extracts (containing endogenous proteins only); lower panel: similar dilutions of Tet-induced extracts were probed with an  $\alpha$ -FLAG antibody. Relative levels of the four FLAG-tagged exosomal factors (indicated on the right) were calculated by quantifying the bands' intensities as above. The separating line between the hRRP40-FLAG and the remaining blots indicates that these were run in separate gels.

(B) The relative cellular levels of endogenous hRRP6, hDIS3, hDIS3L and hRRP40 were calculated by dividing the relative level of each FLAG-tagged protein with its overexpression level from (A).



**Supplementary Figure S5. Relative amounts of cells at 2 and 4 days after second siRNA treatment.** HeLa cells were plated at  $0.5 \times 10^5$  cells/ml in 11ml of DMEM media (without antibiotics). After 24 h cells were treated with the indicated siRNAs and re-transfected after an additional 60 h. One set of plates was counted two days after the second siRNA treatment (grey columns), and a second set of plates was counted after four days (black columns). Standard deviations are shown (n=2). siRNA targeting an unrelated TEL/AML fusion transcript was used as a negative control (C).



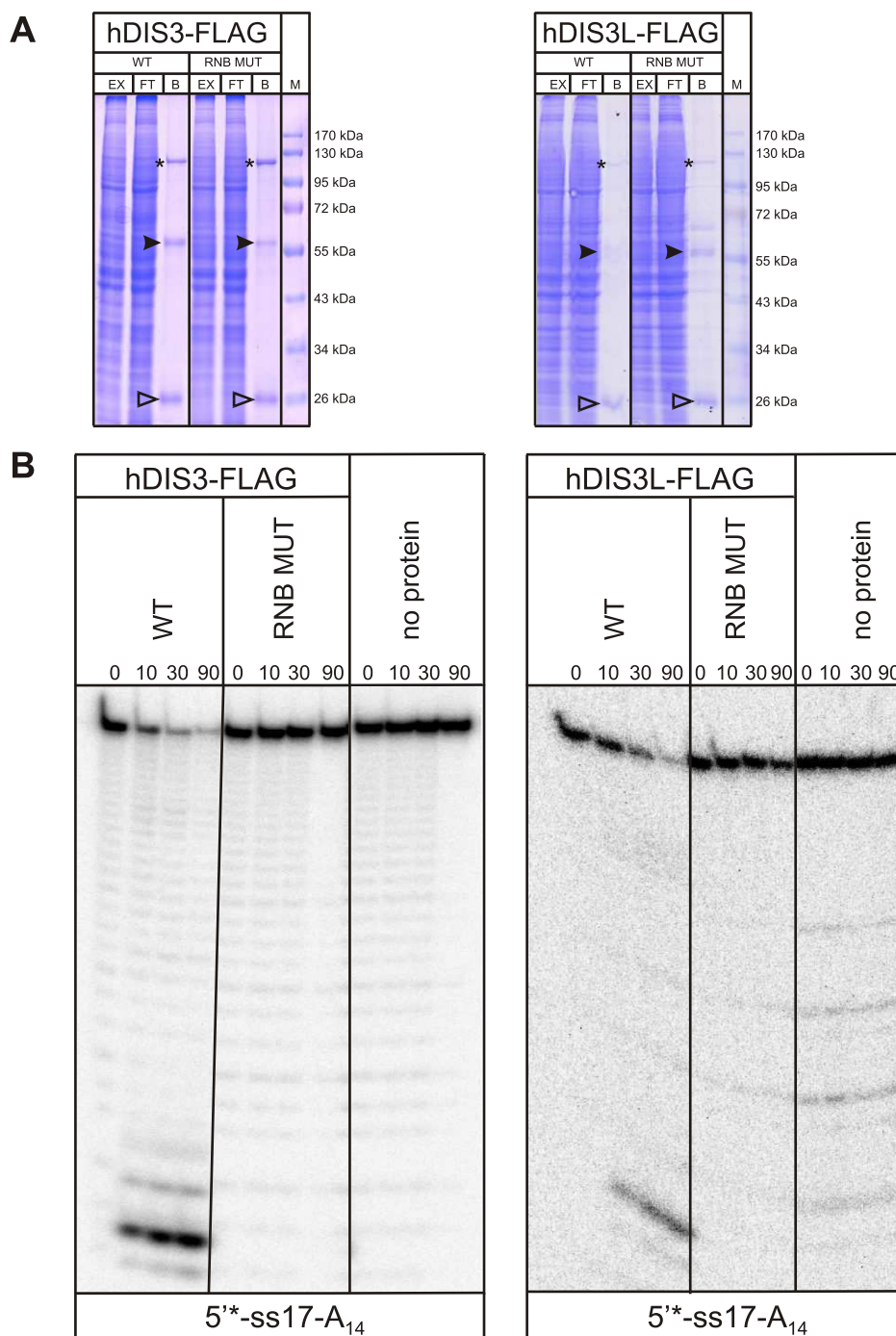
**Supplementary Figure S6. Purification and biochemical analysis of hDIS3 and hDIS3L protein variants expressed in *E. coli*.**

(A) Schematic representations of all expressed proteins: Full-length (FL)-, N-terminal part encompassing the PIN domain (Nterm)- and C-terminal part corresponding to the RNase II/R-homology region (Cterm)-versions of hDIS3 and hDIS3L in their WT form or containing mutation(s) within either their RNB (RNB MUT) or PIN (PIN MUT) domain or in both (DM). Positions of introduced mutations within the catalytic centers of the RNB and PIN domains are indicated by yellow and orange circles, respectively. Note that as WT hDIS3L lacks a conserved aspartic acid in the 140 position corresponding to D146 in hDIS3, another residue (D62) was mutated to create PIN MUT versions of the FL and Nterm proteins.



(B) SDS-PAGE analysis of expressed recombinant proteins. hDIS3 and hDIS3L variants were purified by nickel-column affinity chromatography followed by size exclusion. Protein preparations were loaded on NuPAGE<sup>®</sup> gels together with PageRuler<sup>™</sup> Prestained Protein Ladder as a molecular weight marker. Masses of individual bands are indicated on the right. Positions of bands corresponding to the full length purified proteins are marked with asterisks. Solid arrows indicate degradation products. Open arrow denotes bacterial DnaK chaperone contamination.

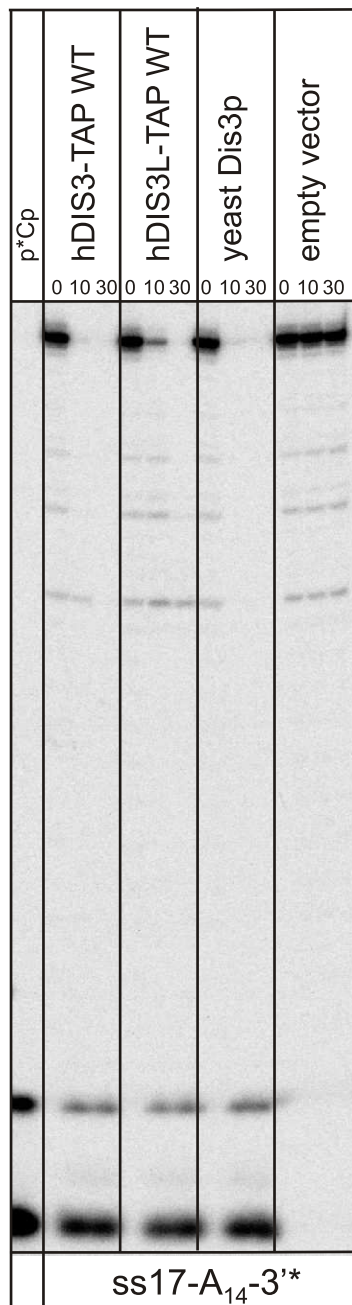
(C and D) Denaturing PAGE and phosphorimaging analysis of products generated after incubation of 5'-labelled ss17-A<sub>14</sub> oligoribonucleotide substrate with the indicated hDIS3 variants or no protein as indicated. Reactions were performed in the presence of 100 μM magnesium and terminated after the time points indicated above the lanes.



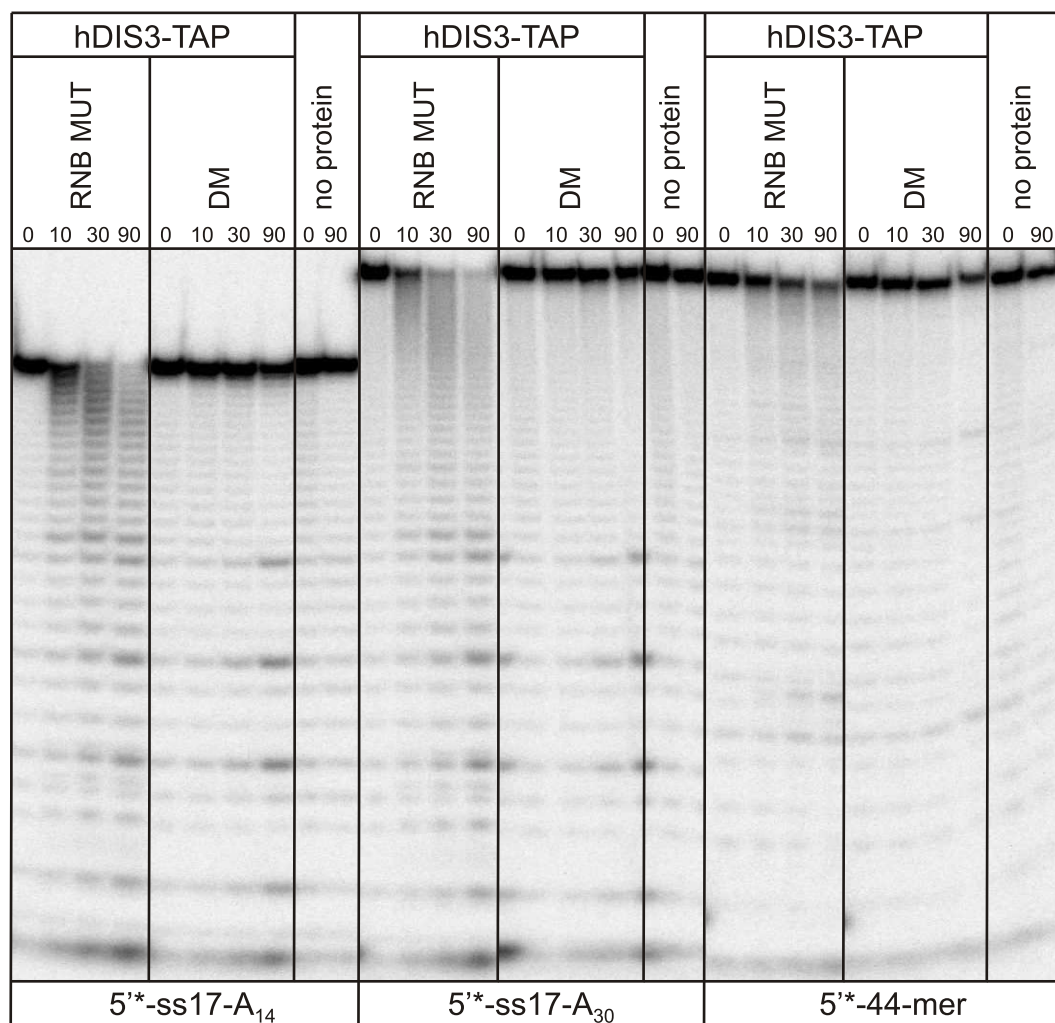
**Supplementary Figure S7. Biochemical analysis of WT and RNB MUT hDIS3 and hDIS3L variants purified from human cells using FLAG epitope.**

(A) SDS-PAGE analysis of hDIS3-FLAG (*left*) and hDIS3L-FLAG (*right*) purifications. Bands corresponding to full length proteins immobilized on anti-FLAG M2 beads are marked with asterisks. Solid and open arrowheads indicate heavy and light chains of anti-FLAG antibodies coupled to the resin, respectively. The identity of proteins bound to the beads was revealed by mass-spectrometry analyses. Column-bound proteins were employed in biochemical experiments shown in (B). Lane designations: EX – native protein extract; FT – flowthrough; B – anti-FLAG resin with bound proteins; M – PageRuler™ Prestained Protein Ladder (Fermentas). Molecular masses of the bands are indicated on the right.

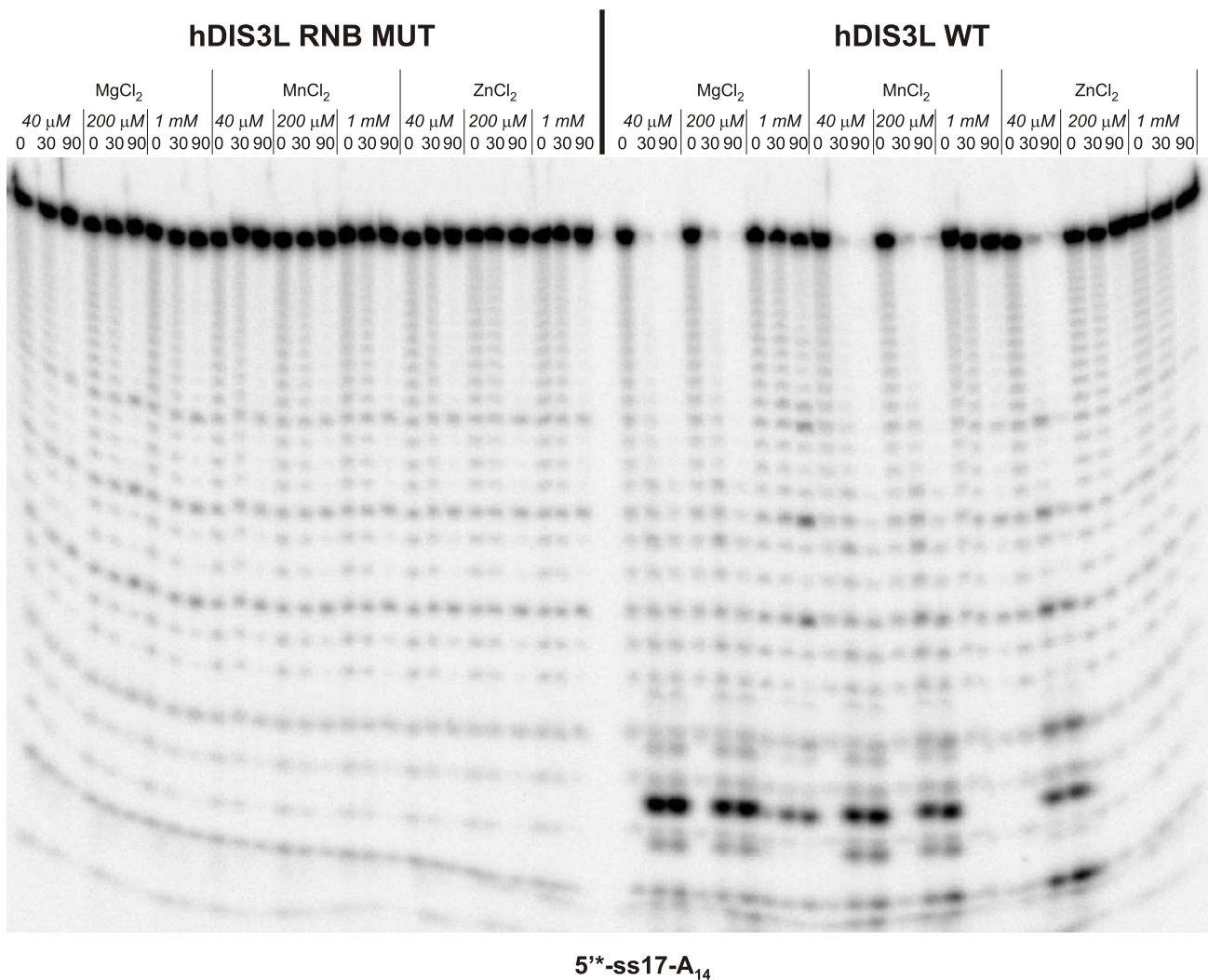
(B) 5'-labelled ss17-A<sub>14</sub> substrate was incubated in a buffer containing 100 μM magnesium with hDIS3-FLAG<sup>WT</sup>/hDIS3-FLAG<sup>RNB MUT</sup> (*left*) or hDIS3L-FLAG<sup>WT</sup>/hDIS3L-FLAG<sup>RNB MUT</sup> (*right*) immobilized on anti-FLAG M2 beads or in the absence of added protein. Samples were collected at the indicated time points and analyzed by denaturing PAGE and phosphorimaging.



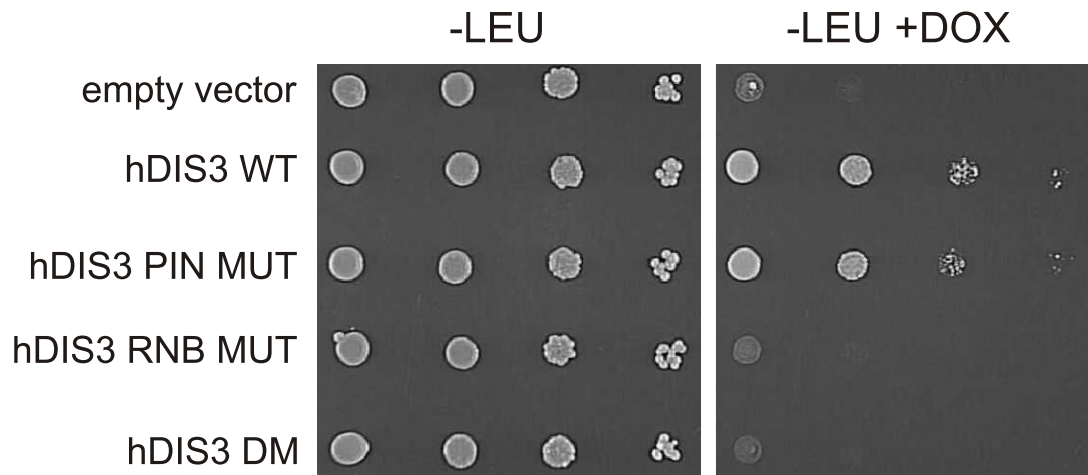
**Supplementary Figure S8. hDIS3 and hDIS3L release mononucleotide as a major terminal degradation product with 3'-labelled substrate.** ss17-A<sub>14</sub> substrate labelled at the 3'-end with [<sup>32</sup>P]pCp was incubated in a buffer containing 100 μM magnesium with hDIS3<sup>WT</sup>, hDIS3L<sup>WT</sup>, yeast Dis3p or an “empty vector”. Reactions were terminated at the indicated time points followed by denaturing PAGE and phosphorimaging. pCp used for the substrate labeling was employed as a molecular weight marker. Final hDIS3, hDIS3L and Dis3p protein concentrations were 0.25 μM, 0.04 μM and 0.2 μM, respectively.



**Supplementary Figure S9. Degradation of different oligonucleotide substrates by hDIS3 PIN domain endoribonuclease activity.** 5'-labelled ss17-A<sub>14</sub>, ss17-A<sub>30</sub> or ss44 RNA substrates were incubated with hDIS3<sup>RNB MUT</sup>, hDIS3<sup>DM</sup> or in the absence of protein, in a buffer containing 3 mM manganese. Reactions were terminated at the indicated time points followed by denaturing PAGE and phosphorimaging. The final hDIS3 protein concentration was 0.25  $\mu$ M.



**Supplementary Figure S10. hDIS3L PIN domain does not display nucleolytic activity, irrespective of the reaction conditions.** 5'-labelled linear ss17-A<sub>14</sub> RNA substrates was incubated with hDIS3<sup>RNB MUT</sup> or hDIS3<sup>WT</sup>, in various buffers containing magnesium, manganese or zinc cations at different concentrations, as indicated. Reactions were terminated at the indicated time points followed by denaturing PAGE and phosphorimaging. hDIS3<sup>RNB MUT</sup> is inactive in all cases, while hDIS3<sup>WT</sup> has only exoribonuclease activity, which is most robust with magnesium as a cofactor and inhibited at higher concentrations of divalent cations. The final hDIS3L protein concentration was 0.04 μM.



**Supplementary Figure S11. Complementation of yeast Dis3p by hDIS3 is strictly dependent on its exonuclease activity.** LEU-marked plasmids bearing the indicated mutant versions of *hDIS3* or an empty vector control were transformed into a yeast strain harboring endogenous *DIS3* under control of a doxycycline repressible promoter. Growth phenotypes of the resulting strains were analyzed in the absence (-LEU, endogenous *DIS3* expressed) or presence (-LEU +DOX, endogenous *DIS3* repressed) of doxycycline.

## Supplementary Tables

**Supplementary Table S1.** hRRP41 Co-IP full data list sorted by SILAC ratio.

Protein	Accession number	Peptides	Protein intensity/MW	Specific	SILAC ratio	Standard deviation (SILAC)	Protein score
hRRP42	IPI00014198.2	10	22576	x	21,61	20,7	532
hCSL4	IPI00032823.1	5	11333	x	21,02	13,6	252
hRRP41	IPI00745613.1	11	46789	x	20,33	20,9	637
hRRP4	IPI00304925.5	11	35262	x	19,00	16,7	690
hRRP45	IPI00029697.3	8	24203	x	18,00	5,7	520
hMPP6	IPI00016074.1	3	7136	x	14,52	4,2	95
hRRP40	IPI00015956.3	6	12541	x	14,30	5,6	242
hMTR4	IPI00647217.2	21	8687	x	13,68	6,8	1103
hRRP46	IPI00015955.5	6	13776	x	13,56	12,8	270
hRRP6	IPI00009464.1	20	12195	x	12,10	4,6	944
hMTR3	IPI00073602.1	4	10712	x	10,13	3,8	170
hDIS3L	IPI00291003.6	1	78	x	9,65	2,1	71
LOC435309	IPI00036267.3	1	240308	x	8,24	1,8	15
hRRP43	IPI00552920.2	10	31743	x	7,83	3,5	506
RPL11	IPI00376798.3	7	53804	x	5,78	10,6	357
SHMT2	IPI00002520.1	1	290	x	5,38	1,2	46
JAK1	IPI00784013.1	2	633	x	3,17	3,4	100
GTPBP4	IPI00385042.4	2	524	x	2,78	0,7	97
HNRNPU	IPI00479217.1	9	10030	x	2,70	4,2	381
RPL34	IPI00219160.3	4	28773	x	2,54	0,6	128
RPL30	IPI00219156.7	7	34402	x	2,31	0,6	342
RPL18A	IPI00026202.1	5	9870	x	2,27	0,7	227
RPL22	IPI00219153.4	2	25177	x	2,15	0,4	131
RPLP0	IPI00008530.1	1	2700	x	2,15	0,5	38
RPL32	IPI00395998.5	4	19273	x	2,12	0,5	162
RPLP1	IPI00412779.2	1	49188	x	2,12	0,5	52
ISOFORM 2							
RPL10	IPI00853161.1	6	11832	x	2,11	0,5	219
RPL10A	IPI00412579.6	2	2885	x	2,10	0,5	83
RPL14	IPI00555744.6	6	21333	x	2,10	0,5	294
RPL24	IPI00306332.4	3	9934	x	2,09	0,5	141
RPL27	IPI00219155.5	4	36695	x	2,09	0,5	105
RPL13A	IPI00304612.9	5	19435	x	2,05	0,5	176
RPL3	IPI00550021.4	15	23109	x	2,04	0,5	596
RALY	IPI00011268.2	3	2588	x	2,03	0,4	110
RPL28	IPI00182533.5	9	29721	x	1,98	0,5	230
RPL6	IPI00329389.8	11	24384	x	1,98	0,5	495
RPLP0	IPI00556485.2	7	19579	x	1,98	0,7	389
RPLP2	IPI00008529.1	5	61949	x	1,97	0,5	278
CORO1B	IPI00007058.1	1	534	x	1,97	0,4	51
RPL17	IPI00413324.6	4	11358	x	1,95	0,5	198
RPL9	IPI00031691.1	4	23447	x	1,94	0,4	198
RPL15	IPI00470528.5	4	14870	x	1,93	0,5	187
RPL37A	IPI00414860.6	4	10935	x	1,93	0,5	197



RPL19	IPI00025329.1	5	9453	x	1,92	0,5	233
ACTG1	IPI00021440.1	1	13485	x	1,92	0,4	119
RPL18	IPI00215719.6	6	35049	x	1,91	0,5	305
RPL7	IPI00030179.3	9	23534	x	1,90	0,5	376
HSPA8	IPI00003865.1	11	8201	x	1,89	0,5	635
RPL21	IPI00247583.5	6	17664	x	1,89	0,6	264
RPL36AL	IPI00056494.5	2	8238	x	1,89	0,4	82
RPL12	IPI00024933.3	5	12167	x	1,87	0,4	258
RPL7A	IPI00299573.12	10	27433	x	1,87	0,5	507
RPL27A	IPI00456758.4	4	29534	x	1,86	0,4	179
RPL4	IPI00003918.6	13	19973	x	1,86	0,5	521
HNRPM	IPI00171903.2	9	5671	x	1,85	0,5	471
RPL26	IPI00027270.1	6	17855	x	1,85	0,4	219
RPLP1	IPI00008527.3	2	19904	x	1,85	0,5	83
RPL13	IPI00465361.4	7	30794	x	1,83	0,4	314
RPL38	IPI00215790.6	2	15687	x	1,81	0,4	75
RPL8	IPI00012772.8	8	11848	x	1,79	0,4	326
LOC285053	IPI00472864.2	1	1645	x	1,78	0,4	17
LOC651825	IPI00735961.2	1	12213	x	1,77	0,4	19
RPL31	IPI00026302.3	5	29330	x	1,75	0,4	185
RPL5	IPI00000494.6	11	14928	x	1,75	0,8	324
U2AF1	IPI00005613.3	1	948	x	1,75	0,4	67
RBM39	IPI00163505.2	1	375	x	1,74	0,4	48
RPL29	IPI00419919.5	3	7796	x	1,72	0,5	93
CFL1	IPI00012011.6	7	19722	x	1,72	0,5	331
RPL23	IPI00010153.5	1	1236	x	1,71	0,4	47
NPM1	IPI00220740.1	7	8528	x	1,68	0,5	239
THOC4	IPI00328840.9	1	665	x	1,65	0,4	34
RPL35A	IPI00029731.8	1	1467	x	1,62	0,4	48
SNRPD2	IPI00017963.1	9	57962	x	1,61	0,4	380
CSDA	IPI00031801.4	1	1465	x	1,59	0,4	99
SF3B14	IPI00032827.1	3	9560	x	1,59	0,4	230
RUVBL2	IPI00009104.7	2	442	x	1,57	0,4	95
SNRPB2	IPI00029267.1	2	1029	x	1,57	0,4	86
U2AF2	IPI00031556.7	1	438	x	1,57	0,4	45
HNRNPC	IPI00216592.2	8	21397	x	1,55	0,8	436
CFL2	IPI00413344.3	2	3254	x	1,55	0,4	51
SLC25A5	IPI00007188.5	3	4578	x	1,52	0,4	153
SNRPD1	IPI00302850.4	4	57377	x	1,52	0,4	253
EIF3D	IPI00006181.1	5	3543	x	1,51	0,8	150
RBM17	IPI00176706.1	3	1643	x	1,50	0,4	146
SF3A3	IPI00029764.1	8	4347	x	1,48	0,5	427
ARPC5L	IPI00414554.5	1	1660	x	1,47	0,3	66
BAT2	IPI00010700.2	2	180	x	1,47	0,5	80
CORO1C	IPI00867509.1	22	43301	x	1,47	0,4	1188
SF3A1	IPI00017451.1	7	2457	x	1,46	0,4	264
RPS24	IPI00219486.2	4	33802	x	1,45	0,4	223
RPS29	IPI00182289.6	1	20516	x	1,45	0,3	48
STK38	IPI00027251.1	22	49188	x	1,45	0,4	1105
XRCC5	IPI00220834.8	1	315	x	1,45	0,3	50
RPS8	IPI00216587.9	12	47838	x	1,44	0,5	678
ACTB	IPI00021439.1	23	497776	x	1,44	0,4	1577
RPS25	IPI00012750.3	6	93908	(x)	1,43	0,3	261

CALM3	IPI00075248.11	3	17054	(x)	1,43	0,4	152
RPS12	IPI00847579.1	6	42605	(x)	1,42	0,3	441
BAT2D1	IPI00083708.2	1	38	(x)	1,42	0,3	24
TWF1	IPI00183508.3	5	2804	(x)	1,42	0,4	270
RPS23	IPI00218606.7	5	44317	(x)	1,42	0,3	230
RPL23A	IPI00021266.1	4	24446	(x)	1,41	0,8	195
TUBB	IPI00011654.2	9	4543	(x)	1,41	0,4	410
TMOD3	IPI00005087.1	7	10060	(x)	1,41	0,4	406
RPS15A	IPI00221091.9	4	23064	(x)	1,40	0,3	167
DHX9	IPI00844578.1	9	1611	(x)	1,40	0,4	363
RPS9	IPI00221088.5	14	45194	(x)	1,40	0,6	530
HSPA1A	IPI00304925.5	21	27223	(x)	1,39	0,3	1124
EIF3F	IPI00654777.2	7	9058	(x)	1,38	0,3	434
RPS19	IPI00215780.5	8	68652	(x)	1,38	0,3	386
DDX21	IPI00477179.1	5	1467	(x)	1,37	0,3	182
RPS16	IPI00221092.8	9	62402	(x)	1,37	0,4	397
RPS6	IPI00021840.1	7	19183	(x)	1,37	0,4	227
RPS21	IPI00017448.1	6	55930	(x)	1,36	0,3	339
TUBA1C	IPI00166768.3	4	4717	(x)	1,36	0,4	273
RPS18	IPI00013296.3	13	76080	(x)	1,36	0,3	553
DHX15	IPI00396435.3	9	4361	(x)	1,35	0,3	498
RPS13	IPI00221089.5	6	27232	(x)	1,35	0,3	240
RPS17	IPI00221093.7	7	31363	(x)	1,35	0,4	283
CAPZB	IPI00642256.2	7	9489	(x)	1,34	0,3	291
SPTAN1	IPI00744706.2	27	2260	(x)	1,34	0,7	1334
EIF3H	IPI00647650.3	5	4064	(x)	1,34	0,3	255
ARPC5	IPI00007280.9	1	1910	(x)	1,33	0,3	66
RPS3A	IPI00419880.6	15	27652	(x)	1,33	0,3	520
EIF3B	IPI00396370.5	13	6703	(x)	1,33	0,3	706
AMD1	IPI00016708.2	1	310	(x)	1,33	0,3	41
ARPC2	IPI00005161.3	2	1705	(x)	1,33	0,3	67
GNB2L1	IPI00641950.3	12	19359	(x)	1,33	0,3	681
RPSA	IPI00413108.4	13	54686	(x)	1,32	0,3	659
SF3B3	IPI00300371.5	19	3999	(x)	1,32	0,3	971
ACTA1	IPI00021428.1	1	1367	(x)	1,31	0,3	59
SF3B1	IPI00026089.3	17	3696	(x)	1,31	0,4	892
EIF3EIP	IPI00465233.1	13	5631	(x)	1,31	0,3	620
PSMA4	IPI00299155.5	1	798	(x)	1,30	0,3	54
RPS20	IPI00012493.1	5	22671	(x)	1,29	0,1	171
ILF3	IPI00298788.4	2	536	(x)	1,29	0,3	73
EIF3E	IPI00013068.1	5	2350	(x)	1,29	0,3	151
SNFPF	IPI00220528.6	1	3590	(x)	1,29	0,3	90
RPS3	IPI00011253.3	17	55517	(x)	1,28	0,3	713
SR140	IPI00143753.6	9	2304	(x)	1,28	0,3	449
RPS11	IPI00025091.3	10	26386	(x)	1,28	0,4	337
XRCC6	IPI00644712.4	2	650	(x)	1,28	0,3	135
SF3B4	IPI00017339.1	2	1884	(x)	1,28	0,3	145
EIF3C	IPI00016910.1	10	3840	(x)	1,28	0,3	579
SF3B2	IPI00221106.5	12	3791	(x)	1,27	0,4	380
EIF3I	IPI00012795.3	6	6778	(x)	1,26	0,3	267
EIF3K	IPI00033143.1	3	4599	(x)	1,26	0,3	145
RBM10	IPI00375731.1	40	59627	(x)	1,26	0,3	2059
RPS5	IPI00008433.4	4	15402	(x)	1,26	0,3	214

RPS27A	IPI00179330.6	1	2985	(x)	1,25	0,3	21
CMBL	IPI00383046.3	2	830	(x)	1,25	0,3	68
RPS26L	IPI00186712.5	6	37258	(x)	1,25	0,5	237
RPS4X	IPI00217030.10	16	38106	(x)	1,25	0,4	813
RPS10	IPI00008438.1	7	31655	(x)	1,25	0,4	372
EIF3A	IPI00029012.1	25	3916	(x)	1,24	0,3	907
EIF3M	IPI00102069.5	6	3282	(x)	1,24	0,3	211
LARP1	IPI00185919.3	2	223	(x)	1,24	0,3	76
BMS1	IPI00006099.1	7	724	(x)	1,24	0,4	374
LIMA1	IPI00008918.1	11	5363	(x)	1,24	0,3	638
EEF1A1L3	IPI00472724.1	7	5364	(x)	1,23	0,5	252
SNRPE	IPI00029266.1	1	7352	(x)	1,22	0,3	60
CALR	IPI00020599.1	1	637	(x)	1,21	0,3	86
STK38L	IPI00237011.5	8	9787	(x)	1,20	0,3	334
EIF3G	IPI00290460.3	8	6043	(x)	1,19	0,3	316
RPS7	IPI00013415.1	3	18713	(x)	1,19	0,3	124
SPTBN1	IPI00005614.6	22	1630	(x)	1,19	0,3	1000
SNRPD3	IPI00017964.1	7	97682	(x)	1,18	0,8	406
SPIN1	IPI00550655.4	8	9654	(x)	1,18	0,3	360
RPS14	IPI00026271.5	5	25835	(x)	1,17	0,3	243
DDX3X	IPI00215637.5	1	116	(x)	1,16	0,3	55
RPS15	IPI00216153.7	4	5235	(x)	1,15	0,3	166
PRPF19	IPI00004968.1	2	965	(x)	1,15	0,3	69
HSPA5	IPI00003362.2	13	4327	(x)	1,14	0,4	653
HSP90AB1	IPI00414676.6	4	1215	(x)	1,14	0,3	172
NAP1L1	IPI00023860.1	4	2974	(x)	1,13	0,3	188
EPB41L3	IPI00032230.2	9	1546	(x)	1,12	0,3	470
ASCC3L1	IPI00420014.2	12	948	(x)	1,12	0,3	510
PRPF31	IPI00292000.6	18	20971	(x)	1,11	0,3	922
EFTUD2	IPI00003519.1	10	2044	(x)	1,11	0,3	489
HIST1H4H	IPI00453473.6	7	33126	(x)	1,11	0,3	374
PRPF8	IPI00007928.4	8	577	(x)	1,09	0,3	301
P4HB	IPI00010796.1	6	2266	(x)	1,08	0,3	262
EIF4B	IPI00012079.1	37	46260	(x)	1,07	0,3	1554
MYO5B	IPI00479962.4	4	163	(x)	1,06	0,4	184
TPP2	IPI00020416.8	1	99	(x)	1,06	0,2	94
HIST1H2BL	IPI00018534.4	4	32765	(x)	1,02	0,3	160
EIF3J	IPI00290461.3	3	1984	(x)	0,99	0,3	106
RCL1	IPI00642256.2	1	415	(x)	0,99	0,3	42
CLNS1A	IPI00004795.1	8	91351	(x)	0,99	0,3	587
HIST1H2AE	IPI00026272.2	3	14143	(x)	0,96	0,2	100
VIM	IPI00418471.6	36	60441	(x)	0,94	0,2	1802
WDR77	IPI00647794.2	14	277402	(x)	0,94	0,3	990
RNPS1	IPI00033561.3	2	1430	(x)	0,94	0,3	107
HIST2H3C	IPI00171611.7	1	1596	(x)	0,91	0,2	22
PPIA	IPI00419585.9	1	356	(x)	0,91	0,2	36
RIOK1	IPI00171336.3	17	10485	(x)	0,90	0,2	874
MIF	IPI00293276.10	1	1080	(x)	0,89	0,2	37
ROCK1	IPI00022542.1	2	112	(x)	0,88	0,4	84
SNRPB	IPI00027285.1	8	41453	(x)	0,85	0,3	394
PRMT5	IPI00441473.3	44	322281	(x)	0,83	0,2	2577
PRPSAP2	IPI00003168.1	12	8992	(x)	0,82	0,2	595
BOLA2B	IPI00410226.3	3	16554	(x)	0,80	0,2	198

FLNA	IPI00302592.2	8	355	(x)	0,77	0,3	415
MYO1C	IPI00010418.4	2	213	(x)	0,77	0,2	137
KIF11	IPI00305289.2	37	10343	(x)	0,56	0,1	2021
GSN	IPI00026314.1	7	734	(x)	0,39	0,1	324
IGHG1	IPI00470657.1	5	955	(x)	0,16	0,2	256

*x*: Indicates that the protein is found in the experiment with a SILAC ratio above background. (x): Indicates that the protein is found in the experiment, but with a SILAC ratio below background.

To be able to compare protein intensities, the intensities are normalized to protein size (MW), since a large protein will contain more Arg or Lys containing peptides, than a smaller. The protein intensity/MW is calculated by summing the intensity of the heavy labelled peptides originating from a specific protein, and dividing this value with the molecular weight.

Proteins with a SILAC ratio above  $1 + 2 \times$  average standard dev (for all proteins identified in this experiment) are believed to be true interaction partners.

The "Protein score" is the summed peptide scores for a given protein

**Supplementary Table S2.** hDIS3 Co-IP full data list sorted by SILAC ratio.

Protein	Accession number	Peptides	Protein intensity/MW	Specific	SILAC Ratio	Standard deviation (SILAC)	Protein score
DDEFL1	IPI00152667.3	1	304	x	100,50	52	4
hRRP44	IPI00746351.2	20	2014	x	31,59	16,35	858
hRRP45	IPI00029697.3	2	136	x	5,85	3,03	101
hRRP46	IPI00644775.1	3	240	x	5,64	2,92	74
hCSL4	IPI00032823.1	3	242	x	5,37	2,78	74
hRRP4	IPI00015905.1	4	293	x	5,23	2,71	80
hRRP41	IPI00745613.2	1	62	x	5,16	2,67	30
hRRP6	IPI00009464.1	6	133	x	4,65	2,41	216
hRRP42	IPI00014198.2	3	117	x	4,56	2,36	159
hRRP43	IPI00552920.2	2	58	x	2,98	1,54	38
hMTR4	IPI00647217.2	10	159	x	2,93	1,52	326
STUB1	IPI00025156.4	1	18	x	2,11	1,09	84
ITM2B	IPI00031821.1	1	86	x	2,05	1,06	58
HSPA8	IPI00003865.1	33	3205	(x)	1,65	0,85	1396
PSMA4	IPI00299155.5	1	38	(x)	1,57	0,81	59
HSPA1A	IPI00304925.5	30	4539	(x)	1,51	0,78	1269
SLC25A5	IPI00007188.5	7	650	(x)	1,39	0,72	309
STK38	IPI00027251.1	11	644	(x)	1,32	0,69	373
EIF4G1	IPI00384463.3	7	79	(x)	1,29	0,68	280
LARP1	IPI00185919.3	7	41	(x)	1,29	0,67	294
TUBB	IPI00011654.2	11	608	(x)	1,26	0,66	508
RPL30	IPI00219156.7	5	2071	(x)	1,23	0,64	204
RPL14	IPI00555744.6	8	1695	(x)	1,23	0,66	339
RPS27A	IPI00179330.6	2	304	(x)	1,22	0,67	56
EIF3M	IPI00102069.5	22	882	(x)	1,22	0,66	863
RPL24	IPI00306332.4	7	2411	(x)	1,19	0,66	322
HNRPF	IPI00003881.5	3	115	(x)	1,17	0,66	135
RUVBL2	IPI00009104.7	4	106	(x)	1,16	0,61	208
RPS15A	IPI00221091.9	9	4575	(x)	1,15	0,7	314
RUVBL1	IPI00021187.4	3	72	(x)	1,15	0,7	132
RPL9	IPI00031691.1	5	3108	(x)	1,15	0,81	168
HSPA5	IPI00003362.2	11	291	(x)	1,15	0,62	519
RPS21	IPI00017448.1	19	16159	(x)	1,15	0,65	822
SERBP1	IPI00410693.3	2	213	(x)	1,15	0,8	48
CFL1	IPI00012011.6	11	2433	(x)	1,15	0,7	427
ACTA1	IPI00021428.1	7	2602	(x)	1,14	0,72	141
EIF3E	IPI00013068.1	15	1350	(x)	1,14	0,66	701
RPSA	IPI00413108.4	25	7115	(x)	1,13	0,65	803
EIF3EIP	IPI00465233.1	26	1467	(x)	1,13	0,64	864
ACTB	IPI00021439.1	46	17	(x)	1,13	0,67	1876
RPS11	IPI00025091.3	10	4289	(x)	1,13	0,65	315
RPS17	IPI00221093.7	8	2797	(x)	1,13	0,83	280
RPS29	IPI00182289.6	2	3466	(x)	1,13	0,76	84
RPL5	IPI00000494.6	19	2567	(x)	1,13	0,65	682
RPL11	IPI00376798.3	6	1601	(x)	1,13	0,67	211
EIF3C	IPI00016910.1	37	1738	(x)	1,13	0,68	1274
RPS3A	IPI00419880.6	23	5855	(x)	1,13	0,61	894
RPL34	IPI00219160.3	5	1810	(x)	1,12	0,7	117

RPS12	IPI00847579.1	8	6167	(x)	1,12	0,62	262
EIF4A1	IPI00025491.1	17	1406	(x)	1,12	0,71	883
EIF3H	IPI00647650.3	24	2293	(x)	1,12	0,74	986
RPL15	IPI00470528.5	8	652	(x)	1,12	0,72	199
RPL13A	IPI00304612.9	14	3055	(x)	1,12	0,62	362
TUBA1C	IPI00166768.3	7	627	(x)	1,11	0,61	261
RPS10	IPI00008438.1	6	1944	(x)	1,11	0,79	216
SNRPB2	IPI00029267.1	5	832	(x)	1,11	0,71	163
GNB2L1	IPI00641950.3	22	6213	(x)	1,11	0,64	828
RPLP2	IPI00008529.1	15	18245	(x)	1,11	0,82	808
EIF3I	IPI00012795.3	16	1972	(x)	1,10	0,62	446
EIF3B	IPI00396370.5	32	1595	(x)	1,09	0,74	1184
HNRNPC	IPI00216592.2	22	5707	(x)	1,09	0,74	1057
SPTBN1	IPI00005614.6	25	182	(x)	1,09	0,72	826
RPL7	IPI00030179.3	11	1550	(x)	1,08	0,96	400
TPP2	IPI00020416.8	36	716	(x)	1,08	0,71	1379
RPL31	IPI00026302.3	11	6033	(x)	1,08	0,78	257
RPL12	IPI00024933.3	7	2231	(x)	1,08	0,78	256
RPS6	IPI00021840.1	13	3194	(x)	1,08	0,82	482
HNRPM	IPI00171903.2	14	264	(x)	1,07	0,83	519
EIF3A	IPI00029012.1	54	1609	(x)	1,07	0,7	1846
RPS9	IPI00221088.5	21	3694	(x)	1,07	0,69	621
RPS8	IPI00216587.9	13	4983	(x)	1,07	0,93	477
RBM17	IPI00176706.1	13	1012	(x)	1,07	0,89	459
RPL4	IPI00003918.6	24	2434	(x)	1,06	0,87	777
RPL26L1	IPI00007144.1	16	2784	(x)	1,06	0,82	510
RPS19	IPI00215780.5	24	8935	(x)	1,06	0,76	913
NAP1L1	IPI00023860.1	5	512	(x)	1,06	0,92	209
VIM	IPI00418471.6	28	3464	(x)	1,06	0,7	921
RPS23	IPI00218606.7	7	2587	(x)	1,06	0,89	250
RPL27A	IPI00456758.4	7	2601	(x)	1,05	0,75	276
CALM3	IPI00075248.11	3	1316	(x)	1,05	0,92	172
SPTAN1	IPI00744706.2	30	238	(x)	1,05	0,75	1012
SR140	IPI00143753.6	12	280	(x)	1,05	0,92	570
RPL23	IPI00010153.5	3	432	(x)	1,05	0,59	110
RPS4X	IPI00217030.10	22	2784	(x)	1,04	0,71	632
RPLP0	IPI00008530.1	14	2303	(x)	1,04	0,88	493
SF3A1	IPI00017451.1	18	613	(x)	1,04	0,77	547
RPS16	IPI00221092.8	13	3641	(x)	1,04	0,69	425
ROCK1	IPI00022542.1	18	261	(x)	1,04	0,78	597
SF3A3	IPI00029764.1	14	947	(x)	1,04	0,72	460
RPL7A	IPI00299573.12	13	2114	(x)	1,04	0,83	405
EIF3F	IPI00654777.2	10	1051	(x)	1,04	0,91	453
RBM10	IPI00375731.1	34	1608	(x)	1,04	0,82	1257
RPS2	IPI00013485.3	16	2688	(x)	1,04	0,92	463
RPL22	IPI00219153.4	8	2778	(x)	1,03	0,63	366
RIOK1	IPI00171336.3	14	853	(x)	1,03	0,91	541
PRPF31	IPI00292000.6	19	1066	(x)	1,03	0,87	505
ASCC3L1	IPI00420014.2	23	128	(x)	1,02	0,95	883
RPLP1	IPI00008527.3	2	2381	(x)	1,02	0,79	80
CCAR1	IPI00217357.2	22	406	(x)	1,02	0,86	699
RPS5	IPI00008433.4	6	1027	(x)	1,02	0,87	321
RPS18	IPI00013296.3	15	2870	(x)	1,02	0,82	470

SNRPD3	IPI00017964.1	8	5215	(x)	1,02	0,93	230
RPL3	IPI00550021.4	23	1720	(x)	1,02	0,72	740
SF3B14	IPI00032827.1	5	974	(x)	1,02	0,86	243
RBBP4	IPI00328319.8	6	305	(x)	1,01	0,84	210
RPL27	IPI00219155.5	10	2137	(x)	1,01	0,9	199
SNRPD1	IPI00302850.4	7	1645	(x)	1,01	0,87	301
THOC4	IPI00328840.9	3	330	(x)	1,01	0,89	78
EIF3G	IPI00290460.3	12	927	(x)	1,01	0,76	398
SF3B3	IPI00300371.5	25	384	(x)	1,01	0,95	880
PABPC1	IPI00008524.1	13	272	(x)	1,01	0,93	379
RPL19	IPI00025329.1	15	2230	(x)	1,01	0,67	437
RPS13	IPI00221089.5	12	3458	(x)	1,01	0,89	225
DHX9	IPI00844578.1	10	126	(x)	1,00	0,94	343
PRPF19	IPI00004968.1	5	160	(x)	1,00	0,95	141
RPL23A	IPI00021266.1	9	1766	(x)	1,00	0,88	414
SF3B2	IPI00221106.5	30	1172	(x)	1,00	0,87	898
HNRNPU	IPI00479217.1	17	830	(x)	1,00	0,88	622
RPS25	IPI00012750.3	5	2730	(x)	0,99	0,72	218
RPS3	IPI00011253.3	23	4672	(x)	0,99	0,9	765
RPL13	IPI00465361.4	16	2355	(x)	0,99	0,74	448
RPL32	IPI00395998.5	12	3122	(x)	0,99	0,91	362
SPIN1	IPI00550655.4	6	418	(x)	0,99	0,89	192
EFTUD2	IPI00003519.1	28	593	(x)	0,99	0,9	1031
XRCC6	IPI00644712.4	13	271	(x)	0,98	0,92	443
PRPF8	IPI00007928.4	29	136	(x)	0,98	0,93	1048
RPL18	IPI00215719.6	11	2215	(x)	0,98	0,88	340
RAN	IPI00643041.3	1	23	(x)	0,98	0,8	15
CLNS1A	IPI00004795.1	4	676	(x)	0,98	0,85	229
RPS20	IPI00012493.1	15	4803	(x)	0,97	0,93	459
RPL10A	IPI00412579.6	10	1232	(x)	0,97	0,84	258
RPS7	IPI00013415.1	23	5312	(x)	0,97	0,89	805
DDX21	IPI00477179.1	9	205	(x)	0,96	0,66	274
SF3A2	IPI00017341.3	8	429	(x)	0,96	0,93	211
MATR3	IPI00017297.1	7	107	(x)	0,96	0,79	171
HIST1H4H	IPI00453473.6	9	3059	(x)	0,96	0,8	365
RPS28	IPI00719622.1	5	6830	(x)	0,95	0,92	133
ILF3	IPI00298788.4	11	341	(x)	0,95	0,73	444
STK38L	IPI00237011.5	12	45	(x)	0,95	0,76	407
SF3B4	IPI00017339.1	8	312	(x)	0,94	0,81	315
SF3B1	IPI00026089.3	30	623	(x)	0,94	0,9	811
DHX15	IPI00396435.3	13	245	(x)	0,94	0,86	529
RPL6	IPI00329389.8	14	1641	(x)	0,93	0,89	432
EEF1AL3	IPI00472724.1	18	1584	(x)	0,93	0,71	529
RPS14	IPI00026271.5	7	1742	(x)	0,92	0,75	174
PRMT5	IPI00441473.3	70	7636	(x)	0,92	0,72	2225
YWHAE	IPI00000816.1	4	139	(x)	0,91	0,66	155
KIF11	IPI00305289.2	16	239	(x)	0,90	0,6	696
ATP5B	IPI00303476.1	4	27	(x)	0,87	0,56	143
EPB41L3	IPI00032230.2	12	140	(x)	0,86	0,55	454
SNFPF	IPI00220528.6	2	377	(x)	0,85	0,5	47
CCT8	IPI00302925.4	14	307	(x)	0,84	0,52	472
NPM1	IPI00220740.1	13	947	(x)	0,82	0,51	426
HIST2H3C	IPI00171611.7	1	17	(x)	0,82	0,52	37

BOLA2B	IPI00410226.3	5	708	(x)	0,82	0,48	129
CCT2	IPI00297779.7	13	363	(x)	0,81	0,47	460
PRPSAP2	IPI00003168.1	3	40	(x)	0,80	0,45	88
SNRPD2	IPI00017963.1	8	2183	(x)	0,78	0,54	267
MAP1B	IPI00008868.3	9	27	(x)	0,73	0,39	414
SNRPB	IPI00027285.1	11	870	(x)	0,73	0,45	206
FLNA	IPI00302592.2	19	87	(x)	0,72	0,38	645
HIST1H2BL	IPI00018534.4	12	1685	(x)	0,69	0,36	422
VCP	IPI00022774.3	17	312	(x)	0,68	0,35	579
DCD	IPI00027547.2	1	15	(x)	0,36	0,19	6
HIST2H2AA3	IPI00216457.7	8	17	(x)	0,24	0,12	288

*x*: Indicates that the protein is found in the experiment with a SILAC ratio above background. (x): Indicates that the protein is found in the experiment, but with a SILAC ratio below background.

To be able to compare protein intensities, the intensities are normalized to protein size (MW), since a large protein will contain more Arg or Lys containing peptides, than a smaller. The protein intensity/MW is calculated by summing the intensity of the heavy labelled peptides originating from a specific protein, and dividing this value with the molecular weight.

Proteins with a SILAC ratio above  $1 + 2 \times$  average standard dev (for all proteins identified in this experiment) are believed to be true interaction partners.

The "Protein score" is the summed peptide scores for a given protein



**Supplementary Table S3.** hDIS3L Co-IP full data list sorted by SILAC ratio.

Protein	Accession number	Peptides	Protein intensity/MW	Specific	SILAC Ratio	Standard deviation (SILAC)	Protein score
CDYL	IPI00293963.4	1	1157	x	253,27	162,42	3
PICALM	REV_IPI00216184.3	1	1134	x	253,27	162,42	1
DCD	REV_IPI00847892.1	1	6291	x	253,27	162,42	4
FECH	IPI00554589.3	1	51	x	110,48	70,85	9
GIGYF2	IPI00647635.3	12	163	x	11,64	7,46	389
ZNF598	IPI00328737.2	2	6	x	11,61	7,44	25
GRID2	IPI00747494.1	1	4	x	9,48	6,08	13
hDIS3L	IPI00879677.1	40	1723	x	9,02	5,79	1419
EIF4E2	IPI00744211.2	2	57	x	7,33	4,7	62
hRRP41	IPI00745613.2	1	99	x	6,96	4,46	22
hRRP46	IPI00644775.1	8	919	x	6,82	4,38	260
SIPA1L3	IPI00297254.4	1	2	x	6,74	4,32	4
hRRP6	IPI00009464.1	6	81	x	6,74	4,32	220
hRRP45	IPI00029697.3	8	433	x	6,68	4,29	340
hRRP42	IPI00014198.2	7	407	x	6,32	4,06	216
hRRP4	IPI00015905.1	9	568	x	5,96	3,82	328
hRRP40	IPI00015956.3	5	332	x	5,90	3,78	267
hMTR3	IPI00073602.1	1	310	x	5,70	3,65	54
hCSL4	IPI00032823.1	5	504	x	5,31	3,41	148
hRRP43	IPI00552920.2	2	129	x	4,96	3,18	61
hMTR4	IPI00647217.2	6	36	x	4,83	3,1	174
HBS1L	IPI00168609.1	3	28	x	2,33	1,49	117
DCD	IPI00027547.2	1	39	(x)	1,75	1,12	14
HSPA1A	IPI00304925.5	38	2283	(x)	1,69	1,08	1522
hRRP4	IPI00015905.1	9	4864	(x)	1,69	3,82	328
HSPA8	IPI00003865.1	33	1564	(x)	1,60	1,03	1358
EIF3E	IPI00013068.1	17	645	(x)	1,59	1,02	687
EIF3I	IPI00012795.3	14	579	(x)	1,59	1,02	451
EIF3C	IPI00016910.1	27	868	(x)	1,58	1,01	899
EIF3H	IPI00647650.3	23	1164	(x)	1,57	1,01	915
HNRPM	IPI00171903.2	10	84	(x)	1,54	0,99	367
EIF3EIP	IPI00465233.1	23	565	(x)	1,51	0,97	812
EIF3M	IPI00102069.5	17	141	(x)	1,50	0,97	575
RPS12	IPI00847579.1	7	3515	(x)	1,48	0,98	324
EIF3F	IPI00654777.2	9	270	(x)	1,48	0,97	299
EIF3B	IPI00396370.5	32	649	(x)	1,46	0,95	1048
EIF3A	IPI00029012.1	52	885	(x)	1,46	0,94	1683
RPS5	IPI00008433.4	4	422	(x)	1,44	0,95	230
RPS11	IPI00025091.3	9	2973	(x)	1,41	0,93	264
RPS10	IPI00008438.1	5	693	(x)	1,39	0,91	147
RPL30	IPI00219156.7	5	735	(x)	1,39	0,9	165
HNRPF	IPI00003881.5	1	5	(x)	1,36	0,9	64
RPS3A	IPI00419880.6	20	3484	(x)	1,36	0,9	581
RPS19	IPI00215780.5	17	3573	(x)	1,35	0,88	584
SLC25A5	IPI00007188.5	5	230	(x)	1,34	0,94	248
HNRNPC	IPI00216592.2	19	1486	(x)	1,34	0,88	861
RPS29	IPI00182289.6	2	1377	(x)	1,33	0,92	77
RPL24	IPI00306332.4	8	1048	(x)	1,32	0,9	390

RPL34	IPI00219160.3	5	892	(x)	1,31	0,88	116
RPS18	IPI00013296.3	12	2347	(x)	1,31	0,89	408
RPL27	IPI00219155.5	8	1475	(x)	1,30	0,85	169
RPS25	IPI00012750.3	5	2301	(x)	1,29	0,86	225
GNB2L1	IPI00641950.3	18	1454	(x)	1,29	0,9	838
EIF4A1	IPI00025491.1	13	235	(x)	1,28	0,84	683
RPS17	IPI00221093.7	6	507	(x)	1,28	0,91	139
RPS23	IPI00218606.7	6	1835	(x)	1,28	0,98	214
RPS8	IPI00216587.9	10	2328	(x)	1,28	0,85	392
RPSA	IPI00413108.4	18	1530	(x)	1,28	0,88	797
RPS21	IPI00017448.1	18	5784	(x)	1,28	0,88	704
EIF3G	IPI00290460.3	7	692	(x)	1,27	0,85	219
RPL23	IPI00010153.5	3	163	(x)	1,27	0,86	88
SERBP1	IPI00410693.3	4	111	(x)	1,26	0,96	133
RPS27A	IPI00179330.6	4	355	(x)	1,26	0,85	114
RPL10A	IPI00412579.6	6	504	(x)	1,26	0,91	178
RPS9	IPI00221088.5	11	626	(x)	1,26	0,85	409
RPS4X	IPI00217030.10	16	968	(x)	1,25	0,88	581
RPL14	IPI00555744.6	10	676	(x)	1,24	0,9	329
RPS6	IPI00021840.1	16	2338	(x)	1,24	0,85	432
RPS16	IPI00221092.8	13	2011	(x)	1,24	0,84	418
RPS2	IPI00013485.3	11	986	(x)	1,23	0,85	322
RPS7	IPI00013415.1	14	2000	(x)	1,23	0,86	456
RPLP2	IPI00008529.1	13	4370	(x)	1,23	0,87	614
RPS15A	IPI00221091.9	5	1007	(x)	1,22	0,86	123
RPL22	IPI00219153.4	7	628	(x)	1,22	0,87	275
RPS20	IPI00012493.1	8	1484	(x)	1,22	0,87	198
SPIN1	IPI00550655.4	5	199	(x)	1,19	0,95	158
YWHAE	IPI00000816.1	2	41	(x)	1,19	0,89	75
RPL31	IPI00026302.3	7	1491	(x)	1,19	0,87	169
RBM17	IPI00176706.1	12	537	(x)	1,18	0,91	485
RPS3	IPI00011253.3	17	1152	(x)	1,18	0,89	523
RPL11	IPI00376798.3	6	1000	(x)	1,18	1,01	244
SR140	IPI00143753.6	13	166	(x)	1,18	0,93	515
RPS14	IPI00026271.5	4	389	(x)	1,18	0,88	127
RPL3	IPI00550021.4	24	1192	(x)	1,18	0,91	549
SNRPD3	IPI00017964.1	8	2071	(x)	1,15	0,94	280
EIF4G1	IPI00384463.3	4	7	(x)	1,15	0,91	77
STK38	IPI00027251.1	11	266	(x)	1,14	0,85	313
RPL18	IPI00215719.6	4	574	(x)	1,14	1,03	224
RPS28	IPI00719622.1	6	3818	(x)	1,13	0,79	132
RPL26L1	IPI00007144.1	9	1700	(x)	1,13	1,01	257
RPL5	IPI00000494.6	16	1400	(x)	1,13	0,81	556
RPL6	IPI00329389.8	11	1094	(x)	1,13	0,89	340
BOLA2B	IPI00410226.3	10	3640	(x)	1,13	0,85	261
RUVBL1	IPI00021187.4	6	73	(x)	1,13	1,01	192
RPL19	IPI00025329.1	9	642	(x)	1,12	0,85	293
HNRNPU	IPI00479217.1	12	270	(x)	1,12	1,06	411
RPLP0	IPI00008530.1	15	675	(x)	1,12	0,91	500
SF3A1	IPI00017451.1	23	360	(x)	1,11	1,06	590
RPL12	IPI00024933.3	10	915	(x)	1,11	0,99	347
RPL23A	IPI00021266.1	7	739	(x)	1,10	0,97	253
MAP1B	IPI00008868.3	16	36	(x)	1,10	1,02	774

RPL13A	IPI00304612.9	7	687	(x)	1,10	0,97	182
RUVBL2	IPI00009104.7	4	31	(x)	1,10	0,99	215
RPL4	IPI00003918.6	19	1005	(x)	1,09	1,05	553
RPL7A	IPI00299573.12	13	609	(x)	1,09	1	288
RBM10	IPI00375731.1	40	929	(x)	1,09	0,87	1512
TUBB	IPI00011654.2	14	105	(x)	1,08	0,94	440
RPL27A	IPI00456758.4	6	657	(x)	1,08	0,89	231
THOC4	IPI00328840.9	5	175	(x)	1,08	1,05	143
CCT8	IPI00302925.4	10	89	(x)	1,07	0,99	329
RPS13	IPI00221089.5	9	877	(x)	1,07	0,93	292
SPTAN1	IPI00744706.2	39	105	(x)	1,07	1,01	990
RPL15	IPI00470528.5	8	550	(x)	1,07	0,99	207
CCT2	IPI00297779.7	12	133	(x)	1,07	0,93	411
SF3A2	IPI00017341.3	6	127	(x)	1,07	0,9	87
DDX21	IPI00477179.1	5	46	(x)	1,06	0,99	121
SPTBN1	IPI00005614.6	26	72	(x)	1,06	1,03	830
NAP1L1	IPI00023860.1	4	121	(x)	1,05	0,94	192
SF3B14	IPI00032827.1	4	154	(x)	1,04	0,97	160
XRCC6	IPI00644712.4	11	52	(x)	1,04	1,02	322
RPL7	IPI00030179.3	10	555	(x)	1,03	1,03	330
RPL13	IPI00465361.4	19	1197	(x)	1,03	0,89	499
PRPF31	IPI00292000.6	16	289	(x)	1,03	1,03	456
SNRPB2	IPI00029267.1	5	229	(x)	1,03	1,01	131
RIOK1	IPI00171336.3	17	461	(x)	1,02	1,01	570
EEF1AL3	IPI00472724.1	10	241	(x)	1,01	0,92	214
NPM1	IPI00220740.1	5	331	(x)	1,01	1,01	205
RBBP4	IPI00328319.8	5	73	(x)	1,01	0,96	184
CCAR1	IPI00217357.2	15	77	(x)	1,01	1,01	311
SF3A3	IPI00029764.1	16	437	(x)	1,00	0,92	468
DHX9	IPI00844578.1	8	22	(x)	1,00	0,98	265
RPL32	IPI00395998.5	7	1014	(x)	1,00	0,84	173
ILF3	IPI00298788.4	5	45	(x)	0,99	0,93	160
RPL9	IPI00031691.1	3	540	(x)	0,97	0,88	117
ROCK1	IPI00022542.1	15	48	(x)	0,97	0,97	391
SF3B4	IPI00017339.1	5	221	(x)	0,97	0,92	162
VCP	IPI00022774.3	7	57	(x)	0,97	0,93	150
MATR3	IPI00017297.1	5	23	(x)	0,97	0,93	65
DHX15	IPI00396435.3	9	67	(x)	0,95	0,93	216
PRMT5	IPI00441473.3	72	5549	(x)	0,94	0,94	2221
SF3B2	IPI00221106.5	33	558	(x)	0,94	0,99	879
SF3B1	IPI00026089.3	27	281	(x)	0,94	0,92	613
CMBL	IPI00383046.3	1	11	(x)	0,93	0,89	2
PABPC1	IPI00008524.1	4	41	(x)	0,93	0,8	174
PRPF8	IPI00007928.4	21	33	(x)	0,93	0,84	687
EFTUD2	IPI00003519.1	17	113	(x)	0,91	0,75	584
SNRPB	IPI00027285.1	6	383	(x)	0,89	0,97	122
TUBA1C	IPI00166768.3	7	164	(x)	0,89	0,94	311
HIST1H4H	IPI00453473.6	7	654	(x)	0,87	0,86	348
TPP2	IPI00020416.8	28	196	(x)	0,87	0,77	995
HSPA5	IPI00003362.2	17	139	(x)	0,87	0,74	457
VIM	IPI00418471.6	25	762	(x)	0,86	0,78	819
SF3B3	IPI00300371.5	16	74	(x)	0,85	0,74	495
PSMA4	IPI00299155.5	2	31	(x)	0,85	0,72	73

ACTB	IPI00021439.1	1	3	(x)	0,84	0,7	81
STK38L	IPI00237011.5	16	43	(x)	0,83	0,77	445
FLNA	IPI00302592.2	17	35	(x)	0,83	0,69	499
EPB41L3	IPI00032230.2	10	80	(x)	0,80	0,62	216
CFL1	IPI00012011.6	8	532	(x)	0,79	0,58	206
KIF11	IPI00305289.2	22	144	(x)	0,79	0,61	874
OAT	IPI00022334.1	4	27	(x)	0,78	0,6	100
PRPF19	IPI00004968.1	4	112	(x)	0,78	0,61	96
SNRPD1	IPI00302850.4	8	1023	(x)	0,78	0,84	296
CLNS1A	IPI00004795.1	8	354	(x)	0,77	0,59	346
SNRPD2	IPI00017963.1	11	1519	(x)	0,77	0,71	223
HIST2H3C	IPI00171611.7	2	95	(x)	0,72	0,55	29
CALM3	IPI00075248.11	4	371	(x)	0,69	0,49	195
ACTA1	IPI00021428.1	8	1337	(x)	0,69	0,47	191
LARP1	IPI00185919.3	7	7	(x)	0,68	0,53	168
ASCC3L1	IPI00420014.2	19	37	(x)	0,61	0,95	624
SNFPF	IPI00220528.6	1	12	(x)	0,59	0,41	32
HIST1H2BL	IPI00018534.4	22	1016	(x)	0,39	0,25	780
PRPSAP2	IPI00003168.1	2	1	(x)	0,16	0,1	55
HIST2H2AA3	IPI00216457.7	24	1	(x)	0,07	0,05	735

*x*: Indicates that the protein is found in the experiment with a SILAC ratio above background. (*x*): Indicates that the protein is found in the experiment, but with a SILAC ratio below background.

To be able to compare protein intensities, the intensities are normalized to protein size (MW), since a large protein will contain more Arg or Lys containing peptides, than a smaller. The protein intensity/MW is calculated by summing the intensity of the heavy labelled peptides originating from a specific protein, and dividing this value with the molecular weight.

Proteins with a SILAC ratio above  $1 + 2 \times$  average standard dev (for all proteins identified in this experiment) are believed to be true interaction partners.

The "Protein score" is the summed peptide scores for a given protein

**Supplementary Table S4.** Oligonucleotides used in this study. “*r*” before sequence in brackets indicates that the oligo is composed of ribonucleotides.

Oligonucleotide	Sequence	Purpose
SLICD3f	TGATTGAAGTCTACCAGGAACAAACCGGTGGATCCatgctcaagtc Caagacgttc	generation of pHEX1
SLICD3r	CGGATCTCAGTGGTGGTGGTGGTGGTGCTCGAGctattttccaagcttc Atcttc	generation of pHEX1
SLICD3lf	TGATTGAAGTCTACCAGGAACAAACCGGTGGATCCatgctgcagaa Gcgggag	generation of pHEX2
SLICD3lr	CGGATCTCAGTGGTGGTGGTGGTGGTGCTCGAGtcatattccataattgt Ttg	generation of pHEX2
HD3NFor	<u>CTCGAG</u> CACCACCACCACCACCCTGAGATCCG	generation of pHEX3 -pHEX4
HD3NRev	TTATCATTCTTCAGACAAACAAGCAAGACGATCTATG	generation of pHEX3
HD3LNRev	TTACTAAAGGATAGAATCACAAAGCTCGTGGGCAGC	generation of pHEX4
HD3CFor	ATGGGGAATGAAATAGAAAGTGAAAAATAATATTTTCAG	generation of pHEX5
HD3CRev	<u>GGATCC</u> ACCGGTTTGTTCCTGGTAGACTTCAATCACATC	generation of pHEX5 -pHEX6
HD3LCFor	ATGCAGTCTCGACGGGAGAGAGAGAATGAGAGTCAGG	generation of pHEX6
D3PINF	AGGAATA <u>Accgg</u> GCGATTTCGAGTAGCAGCAAATGGTACAATG	site-directed mutagenesis (hDIS3 D146N)
D3PINR	TCGAATCG <u>Ccgg</u> TTATTCTGTTCATTAGCATTCTCCCTG	site-directed mutagenesis (hDIS3 D146N)
D3RNBF	ATGTA <u>CTgat</u> atcAACGATGCTCTACATTGTCGAGAACTCG	site-directed mutagenesis (hDIS3 D487N)
D3RNBR	AGCATCGT <u>Tgat</u> atcAGTACATCCTGGTGGGTCTACACTAC	site-directed mutagenesis (hDIS3 D487N)
D3LPINF	TGATCC <u>Ccaattg</u> GAAAGTTGTTCAAGATTATCTTGAGATCC	site-directed mutagenesis (hDIS3L D62N)
D3LPINR	AACTTTC <u>Ccaattg</u> GGGATCACGTAATGAGTCACATCACTAG	site-directed mutagenesis (hDIS3L D62N)
D3LRNBF	TTGTGA <u>Agacgtc</u> AATGACACACTCTCAGTCAGAACCTTAAATAAT GG	site-directed mutagenesis (hDIS3L D486N)
D3LRNBR	GTGTCAT <u>Tgacgtc</u> TTCACAACCTTTGGGGTCAATGCTGAATACG	site-directed mutagenesis (hDIS3L D486N)
RSZ132	CGAGCAGAAACTCATCTCTGAAGAGGATCTGTAGGCTAGCGG CC	generation of pRS255

RSZ133	GCTAGCCTACAGATCATCTTCAGAGATGAGTTTCTGCTCGGGC C	generation of pRS255
RSZ143	CGATTACAAGGATGACGACGATAAGTAGGCTAGCGGCC	generation of pRS201
RSZ144	GCTAGCCTACTTATCGTCGTCATCCTTGTAATCGGGCC	generation of pRS201
RZS168	<u>GCACTCGAGGGAGGATCCATGGAAAAGAG</u>	generation of pRS72
RSZ169	<u>CTGGGGCCCTCAGGTTGACTTCCCCGCGGA</u>	generation of pRS72
dis3-tap-fw	<u>tgaggtacc</u> ATGCTCAAGTCCAAGACGTTTC	cloning of hDIS3 ORF into pcDNA5/FRT/TO-derived backbones (pRS255, pRS201 and pRS72)
dis3-tap-rv	tgactcgagTTTTCCAAGCTTCATCTTC	cloning of hDIS3 ORF into pcDNA5/FRT/TO-derived backbones (pRS255, pRS201 and pRS72)
dis3l-tap-fw	<u>tgaggtacc</u> ATGCTGCAGAAGCGGGAGAAG	cloning of hDIS3L ORF into pcDNA5/FRT/TO-derived backbones (pRS255, pRS201 and pRS72)
dis3l-tap-rv	tgactcgagTATTCCATAATTGTTTGAAACATC	cloning of hDIS3L ORF into pcDNA5/FRT/TO-derived backbones (pRS255, pRS201 and pRS72)
D3COMPL	<u>gcgtctaga</u> ATGCTCAAGTCCAAGACGTTCTTAAAAAAGACCCGG GCGG	cloning of hDIS3 ORF into p415
D3COMPR	<u>gcgctcgag</u> CTATTTTCCAAGCTTCATCTTCTTTTCTTTGGTCCAT TAAGG	cloning of hDIS3 ORF into p415
D3LCOMPL	<u>ataactagt</u> ATGCTGCAGAAGCGGGAGAAGGTGCTGCTGCTGAGG ACCTTC	cloning of hDIS3L ORF into p415
D3LCOMPR	<u>cgctcgag</u> TCATATTCCATAATTGTTTGAAACATCCAGGAGAGCT AGGTCCCG	cloning of hDIS3L ORF into p415
hD3Fup	<i>ATGgattacaaggatgacgacgataag</i> <u>ATCTGAT</u> CATGTAATTAGTTATG TCACG	generation of pHEX34
hD3Fdown	<u>TCAGAT</u> <i>tctatcgctgctccttgaate</i> CATTTTCCAAGCTTCATCTTC	generation of pHEX34
hD3LPrev	<u>cgctcgag</u> <b>TCAGAT</b> <i>tctatcgctgctccttgaate</i> CATTATTCCATAATTGTT TGAAAC	generation of pHEX35

hRRP6 <i>Bam</i> HI FW	aagcttggatccATGGCGCCACCCAGTACC	generation of pHEX32
hRRP6 FLAG <i>Not</i> I RE	ctctagggggccgcTCATTATCGTCATCGTCTTTGTAGTCTCTCTGTGG CCAGTTGTAC	generation of pHEX32
hRrp41 <i>Bam</i> HI FW	aagcttggatccATGGCGGGGCTGGAGCTCTTG	generation of pHEX33
hRrp41 FLAG <i>Not</i> I RE	ctctagggggccgcTCATTATCGTCATCGTCTTTGTAGTCGTCCCCAG CAAGATAGAGGC	generation of pHEX33
HD3F883	GAAGATATTGTGGCTGTGGAGC	sequencing of hDIS3 constructs
HD3F1848	CCGTGGACTGAATAAACTAGCC	sequencing of hDIS3 constructs
HD3F2429	TGACAGACAAACACAAGCTTGC	sequencing of hDIS3 constructs
HD3R1021	TTACAGCAGTCTTAAGCATTCG	sequencing of hDIS3 constructs
HD3R1592	CTGGCTGATTCTTGATCCAAGG	sequencing of hDIS3 constructs
HD3R2443	TGTGTTTGTCTGTCAACTCTGG	sequencing of hDIS3 constructs
E5rv	AGCGTCCAGATTTAATCCCAGCT	sequencing of hDIS3L constructs
E5fw	ACCTGGACAATTTCTGGCCTGAT	sequencing of hDIS3L constructs
E8fw	CATACTTCAGAAGAACTGGCGGGA	sequencing of hDIS3L constructs
E11fw	CCACTTATTATCTAGCAGATCGTCGC	sequencing of hDIS3L constructs
E13fw	GTCCAATAAAACTGGCTG	sequencing of hDIS3L constructs
E15fw	CAGCACAGCATTCTCAGAAGC	sequencing of hDIS3L constructs
SumoF	TCATACTGTCAAAGACAGGG	amplification and sequencing of inserts in the pET-28M-6xHis-SUMOTag backbone
RTADZ-54	GCTAGTTATTGCTCAGCGG	amplification of inserts in the pET-28M-6xHis-SUMOTag
RSZ-174	TCGTTTAGTGAACCGTCAG	sequencing of inserts in the pcDNA5/FRT/TO backbone
p415-left	GTTTCCTCGTCATTGTTCTCG	sequencing of inserts in the p415 backbone
ss17-A <sub>14</sub>	r(CCCACCACCAUCACUAAAAAAAAAAAAAAAA)	RNA oligonucleotide substrate used in biochemical assays
ss17-A <sub>30</sub>	r(CCCACCACCAUCACUAAAAAAAAAAAAAAAAAAAA AAAAAA)	RNA oligonucleotide substrate used in biochemical assays
ss44	r(CGACUGGAGCACGAGGACACUGACAUGGACUGAAGGAGUA GAAA)	RNA oligonucleotide substrate used in biochemical assays

compl	r(AAGUGAUGGUGGUGGGG)	RNA oligonucleotide used in biochemical assays
GAPDH (FW/RE)	GTCAGCCGCATCTTCTTTTG/GCGCCAATACGACCATC	qPCR primer pair
40-2 (FW/RE)	GGGAGTCTAAGGAAAAGGAG/CAGTGAAAGGAGAGTATC	qPCR primer pair
40-13 (FW/RE)	GGAAATAGTGGAGAAAAGCA/CATTTTTGAAGGAACGGTAG	qPCR primer pair
40-33 (FW/RE)	CTGGCCTAGCTAAAGTCTCA/TCTGCTCCTAGCTCTCAGTC	qPCR primer pair
40-59 (FW/RE)	CTTCTGAAGGGTTTTGTGTC/CGTGGCTTCATAGTC CTTAT	qPCR primer pair
MYC (FW/RE)	TGCAGCCGTATTTCTACTG/TATCTGGAAGAAATTCGAGC	qPCR primer pair
FOS (FW/RE)	GCCTGTCAACGCGCAGGACT/TCCGGTTGCGGCATTTGGCT	qPCR primer pair
dT primer	GGCCACGCGTCGACTAGTACTTTTTTTTTTTTTTTTTTVN	primer for reverse transcription
eGFP siRNA target (control)	GACGUAAACGGCCACAAGU	siRNA-mediated knock down
TEL/AML siRNA target (control)	GGAGAAUAGCAGAAUGCAU	siRNA-mediated knock down
hRRP6 siRNA target	CCAGUUAUACAGACCUAUA	siRNA-mediated knock down
hDIS3 siRNA target	AGGUAGAGUUGUAGGAAUA	siRNA-mediated knock down
hDIS3L siRNA target	CGUAAAGACUUGAGGAAAA	siRNA-mediated knock down
hRRP40 siRNA target	CACGCACAGUACUAGGUCA	siRNA-mediated knock down
5.8S rRNA oligo probe	GTGTCGATGATCAATGTGTCCTGCAATTCA	probe for northern-blot
scR1 oligo probe	ATCCCGGCCGCCTCCATCAC	probe for northern-blot



**Supplementary Table S5.** Plasmids used in this work.

<b>Plasmid</b>	<b>Genotype</b>
pDrK	[pDRIVE (Qiagen) with removed <i>ScaI-NaeI</i> fragment]
pRS255	[pcDNA5/FRT/TO (Invitrogen)] <i>c-myc epitope</i>
pRS201	[pcDNA5/FRT/TO (Invitrogen)] <i>FLAG-tag</i>
pRS72	[pcDNA5/FRT/TO(Invitrogen)] <i>TAP-tag</i>
pHEX1	[pET-28M-6xHis-SUMOTag] <i>hDIS3 FL WT</i>
pHEX2	[pET-28M-6xHis-SUMOTag] <i>hDIS3L FL WT</i>
pHEX3	[pET-28M-6xHis-SUMOTag] <i>hDIS3 Nterm WT</i>
pHEX4	[pET-28M-6xHis-SUMOTag] <i>hDIS3L Nterm WT</i>
pHEX5	[pET-28M-6xHis-SUMOTag] <i>hDIS3 Cterm WT</i>
pHEX6	[pET-28M-6xHis-SUMOTag] <i>hDIS3L Cterm WT</i>
pHEX7	[pET-28M-6xHis-SUMOTag] <i>hDIS3 FL PIN MUT (D146N)</i>
pHEX8	[pET-28M-6xHis-SUMOTag] <i>hDIS3 FL RNB MUT (D487N)</i>
pHEX9	[pET-28M-6xHis-SUMOTag] <i>hDIS3 FL DM (D146N, D487N)</i>
pHEX10	[pET-28M-6xHis-SUMOTag] <i>hDIS3L FL PIN MUT (D62N)</i>
pHEX11	[pET-28M-6xHis-SUMOTag] <i>hDIS3L FL RNB MUT (D486N)</i>
pHEX12	[pET-28M-6xHis-SUMOTag] <i>hDIS3L FL DM (D62N, D486N)</i>
pHEX13	[pET-28M-6xHis-SUMOTag] <i>hDIS3 Nterm PIN MUT (D146N)</i>
pHEX14	[pET-28M-6xHis-SUMOTag] <i>hDIS3 Cterm RNB MUT (D487N)</i>
pHEX15	[pET-28M-6xHis-SUMOTag] <i>hDIS3L Nterm PIN MUT (D62N)</i>
pHEX16	[pET-28M-6xHis-SUMOTag] <i>hDIS3L Cterm RNB MUT (D486N)</i>
pHEX17	[pcDNA5/FRT/TO-myc] <i>hDIS3L WT</i>
pHEX18	[pcDNA5/FRT/TO-FLAG] <i>hDIS3 WT</i>
pHEX19	[pcDNA5/FRT/TO-FLAG] <i>hDIS3L WT</i>
pHEX20	[pcDNA5/FRT/TO-TAP] <i>hDIS3 WT</i>
pHEX21	[pcDNA5/FRT/TO-TAP] <i>hDIS3L WT</i>
pHEX22	[p415] <i>hDIS3 WT</i>
pHEX23	[p415] <i>hDIS3L WT</i>
pHEX24	[p415] <i>hDIS3 RNB MUT (D487N)</i>

pHEX25	[p415] <i>hDIS3 PIN MUT (D146N)</i>
pHEX26	[p415] <i>hDIS3 DM (D146N, D487N)</i>
pHEX27	[pcDNA5/FRT/TO-FLAG] <i>hDIS3 RNB MUT (D487N)</i>
pHEX28	[pcDNA5/FRT/TO-TAP] <i>hDIS3 RNB MUT (D487N)</i>
pHEX29	[pcDNA5/FRT/TO-TAP] <i>hDIS3 DM (D146N, D487N)</i>
pHEX30	[pcDNA5/FRT/TO-TAP] <i>hDIS3L RNB MUT (D486N)</i>
pHEX31	[pcDNA5/FRT/TO-TAP] <i>hDIS3L DM (D62N, D486N)</i>
pHEX32	[pcDNA5/FRT/TO-FLAG] <i>hRRP6</i>
pHEX33	[pcDNA5/FRT/TO-FLAG] <i>hRRP41</i>
pHEX34	[p415] <i>hDIS3 WT-FLAG</i>
pHEX35	[p415] <i>hDIS3L WT-FLAG</i>

### Supplementary references

Lebreton A, Tomecki R, Dziembowski A, Seraphin B (2008) Endonucleolytic RNA cleavage by a eukaryotic exosome. *Nature* **456**: 993-996

Li MZ, Elledge SJ (2007) Harnessing homologous recombination in vitro to generate recombinant DNA via SLIC. *Nat Methods* **4**: 251-256

Malakhov MP, Mattern MR, Malakhova OA, Drinker M, Weeks SD, Butt TR (2004) SUMO fusions and SUMO-specific protease for efficient expression and purification of proteins. *J Struct Funct Genomics* **5**: 75-86

Marshall T, Abbott NJ, Fox P, Williams KM (1995) Protein concentration by precipitation with pyrogallol red prior to electrophoresis. *Electrophoresis* **16**: 28-31

Preker P, Nielsen J, Kammler S, Lykke-Andersen S, Christensen MS, Mapendano CK, Schierup MH, Jensen TH (2008) RNA exosome depletion reveals transcription upstream of active human promoters. *Science* **322**: 1851-1854